PNE 1113

Plowshare civil, industrial and scientific uses for nuclear explosives

UNITED STATES ARMY CORPS OF ENGINEERS

FORT PECK RESERVOIR
MONTANA

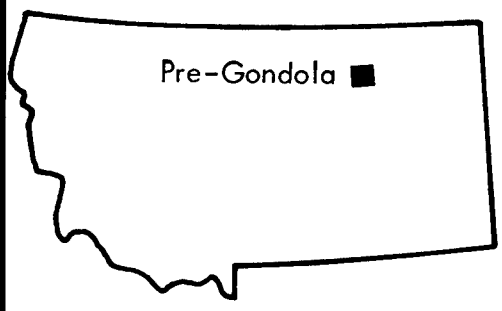

PROJECT
PRE-GONDOLA II

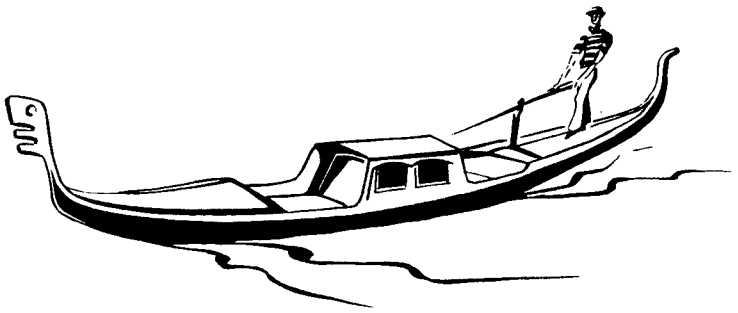

CLOSE-IN GROUND MOTION AND EARTH STRESS

Charles E. Joachim
U. S. Army Engineer Waterways Experiment Station
Vicksburg, Mississippi 39180

U. S. Army Engineer Nuclear Cratering Group
Livermore, California

ISSUED: October 1968

Printed in the United States of America
Available from
Clearinghouse for Federal Scientific and Technical Information
National Bureau of Standards, U. S. Department of Commerce
Springfield, Virginia 22151
Price: Printed Copy ~~$3.00~~; Microfiche ~~$0.65~~

PNE 1113

PROJECT PRE-GONDOLA II

A WET MEDIUM, 140-TON ROW-CHARGE CRATERING EXPERIMENT IN VARYING TERRAIN

CLOSE-IN GROUND MOTION AND EARTH STRESS

Charles E. Joachim

U. S. Army Engineer Waterways
Experiment Station
Vicksburg, Mississippi 39180

October 1968

ABSTRACT

Stress, particle velocity, and acceleration data were obtained from a 140-ton nitromethane row-charge detonation in a saturated clay-shale. The charge row consisted of two 40- and three 20-ton spheres (first and fourth charges were 40 tons) extending S 11 W from the Pre-GONDOLA I Charlie crater on an 80-foot spacing (first charge 105 feet from crater center). The primary instrument line (stress and particle velocity gages) extended S 79 E from the center charge (G) with gage stations 100, 150, 200, 300, and 400 feet from G. Gage depths were 10 and 50 feet except the 400-foot station which was gaged at 50 feet only. Acceleration measurements were made on the slopes of the Pre-GONDOLA I Delta and Charlie craters and at the Control Point (CP).

Peak stress measurements were higher than Pre-GONDOLA I data. As the charge-to-gage distance increased, the individual compressional waves from the various charges began to coalesce. The resulting stresses (coalesced wave) scale using combined charge weights and cube root scaling.

Initial peak horizontal velocity compares well with Pre-GONDOLA I data. Similar to stress, velocities resulting from the coalesced shock front scale using cube root.

A low-amplitude, long-duration acceleration was recorded at the Delta and Charlie craters. The fractured crater material filtered out the high-frequency, high-amplitude motions anticipated at the crater slope and lowered the average propagation velocities. CP accelerations compare well with predictions based on competent media.

PREFACE

This study was performed by the U. S. Army Engineer Waterways Experiment Station (WES) for the U. S. Army Engineer Nuclear Cratering Group (NCG) during the period May-June 1967. Field support was provided by the Fort Peck Area Office, CE, and the Omaha District, CE.

The work was conducted by personnel of the WES Nuclear Weapons Effects Division (NWED) under the direction of Mr. G. L. Arbuthnot, Jr., Division Chief; Mr. L. F. Ingram, Chief, Physical Sciences Branch; and Mr. J. D. Day, Chief, Blast and Shock Section. NWED Project personnel were Messrs. C. E. Joachim and W. M. Gay. Messrs. L. T. Watson and G. H. Williams of the Instrumentation Branch, Technical Services Division, WES, were responsible for the instrumentation. COL John R. Oswalt, Jr., CE, was Director of the WES and Mr. J. B. Tiffany was Technical Director during this work.

CONTENTS

FIGURES

FIGURES

CHAPTER 1

INTRODUCTION

1.1 DESCRIPTION OF PROJECT PRE-GONDOLA II

Project Pre-GONDOLA II was a row-charge cratering experiment in weak, wet clay-shale conducted by the U. S. Army Engineer Nuclear Cratering Group (NCG) as a part of the joint Atomic Energy Commission-Corps of Engineers nuclear excavation research program. The primary purpose of this nominal 140-ton 5-charge row-charge experiment was to gain row-charge cratering experience in a weak, wet medium. In addition, this experiment tested techniques for connecting a row-charge crater to an existing crater and for over-excavating to accept throwout from a follow-on connecting row-charge crater.

Project Pre-GONDOLA II was detonated in Valley County, near the edge of the Fort Peck Reservoir approximately 18 miles south of Glasgow, Montana, at exactly 0800 hours (MDT) 28 June 1967. Coordinates of the center charge were W106 38'31", N47 55'51". The orientation of the row was along a 10 east of north to 10 west of south alignment extending through the center of the Charlie crater.

The average lip-crest to lip-crest dimensions were 640 feet by 280 feet. Individual charge yields, depths, spacing,

and resulting apparent crater dimensions were as follows:

Emplacement Configuration (feet)				Apparent Crater Dimensions (feet)	
Charge	tons NM**	Depth of Burst	Spacing	Width W_a	Depth D_a
Charlie (existing crater)			105.5		
E (connecting crater)	38.61	59.7		206.5	55.5
			79.8		
F	19.70	49.4		152.5	37.5
			79.9		
G (center crater)	19.55	48.8		164.0	36.9
			79.9		
H (over-excavating charge)	39.56	59.9		214.5	57.0
			79.9		
I	20.00	48.8		173.0	33.5

1.2 OBJECTIVES

The primary objective of the study described herein was to obtain close-in (≤400 feet) ground-motion and earth-stress measurements from a row-charge detonation in weak, wet clay-shale. Motion measurements were also performed for the existing Charlie and Delta crater slopes and at the Control Point (CP).

1.3 BACKGROUND

Efficient use of nuclear devices for large-scale excavations requires reasonably precise predictions of initial

** Spherical charges of liquid explosive nitromethane (CH_3NO_2). Actual total charge weight was 137.42 tons.

crater dimensions and subsequent long-term stability. Such predictions can only be made if cratering experience is gained in a wide variety of geologic media, particularly those which might be encountered in excavation projects. The physical measurement of crater parameters together with measurements of transient, directly coupled ground motions and stresses is used to evaluate the engineering properties of the excavated media.

Early cratering experiments were conducted by NCG in dry materials, i.e., basalt, rhyolite, and desert alluvium. Since it is highly probable that some portions of any major excavation will be in material at least partially saturated, cratering data are needed for wet materials. Also, design for long-term use of a canal requires knowledge of slope stability when explosively excavated slopes are subjected to wetting. This includes pore pressure effects of water behind the slopes and erosive effects of water flowing in the channel. The Pre-GONDOLA cratering experiments conducted by NCG at Fort Peck, Montana, provide data for one such medium, a weak, wet clay-shale (known as "Bearpaw" shale).

Due to a lack of meaningful cratering data for these media, it was necessary to conduct a site calibration test series. Pre-GONDOLA I, a series of four, single-charge 20-ton experiments,

was conducted for this purpose. Close-in stress and ground motion measurements were made in conjunction with the Bravo Event of this series[1*]. The data obtained served as a basis for design of this project on Pre-GONDOLA II, a row-charge event. This report describes that portion of the Pre-GONDOLA II experiment concerned with measurement of close-in stress and ground motion.

* Superscript numerals refer to similarly numbered items in References at the end of the text.

CHAPTER 2

PROCEDURE

2.1 EXPERIMENTAL PLAN

The main gage layout for Pre-GONDOLA II is shown in plan and profile in Figure 2.1. A total of nine earth stress gages, and nine horizontal and seven vertical particle velocity gages were installed at nominal depths of 10 and 50 feet and at horizontal distances of 100 to 400 feet. The deep gages (50-foot depth) were located along a line perpendicular to the charge row at charge G. The shallow gages (10-foot depth) were installed in separate holes located 10 feet north of and perpendicular to the main gage line. In addition to the main gage line, surface accelerometers were placed on the existing Charlie and Delta crater slopes (Figure 2.2) to measure motion of the slopes, and surface accelerometers were placed at the CP. Table 2.1 lists the main line instrumentation by gage type and location and also gives predicted peak values. Table 2.2 lists all accelerometers, and gives peak predicted values.

2.2 PREDICTIONS

Because of the uniqueness of the experiment there was no empirical basis for predicting stresses and motions. Although close-in earth motions from multiple contained bursts in a

linear array have been measured[2], these measurements were made in an entirely different material (dry basalt) and in line with the charges rather than normal to the array as planned for Pre-GONDOLA II. Therefore, predictions were based on stress and velocity measurements obtained from the 20-ton single-charge calibration series (Event Bravo). Based on these measurements, stress and horizontal particle velocity inputs from the individual charges of the row were computed for each of the nine gage locations. Cube-root scaling from Bravo was used to obtain the 40-ton charge inputs. Applying the principle of superposition, peak values which occurred within any 10-msec time interval were added. The maximum values thus obtained were used for instrument set-range predictions (Table 2.1). These predictions were considered conservative because, in this procedure, no allowance or consideration was made for the signal decay.

Peak particle velocity predictions were based on radial measurements from Pre-GONDOLA I[1]. Using these data, vertical and horizontal particle velocity predictions were computed from the following relations:

$$u_H = u_R \cos \theta$$

$$u_V = u_R \sin \theta$$

where

u_R = radial particle velocity

u_H = horizontal particle velocity

u_V = vertical particle velocity

θ = angle between horizontal and charge-gage line

Particle velocities up to 1/3 u_R have been measured perpendicular to the compressional wave propagation although wave propagation theory does not predict these motions. Therefore, the minimum vertical particle velocity prediction used was 1/3 u_R.

No acceleration data were available on crater slopes; therefore, predictions (Table 2.2) were made using the following equation taken from Newmark[3], based on continuous media.

$$A_R = 2\ u_R/t_R$$

where

A_R = radial acceleration

u_R = radial particle velocity

t_R = rise time to peak radial particle velocity

This equation is derived for rock, primarily from tests conducted at the Nevada Test Site.

The peak radial particle velocity obtained from the 20-ton Bravo Event was used in this equation. It was assumed that the

single charge nearest the gage would contribute the maximum ground motion input at that gage location due to the unsymmetrical gage-charge geometry (Figure 2.2).

The range of rise times given by Newmark is 1/6 to 1/12 of the arrival time. A rise time of one-twelfth the arrival time was used in making these predictions. This method gave the highest peak acceleration prediction and was the more conservative approach. Peak vertical accelerations were predicted using the same method used for peak vertical particle velocity.

2.3 INSTRUMENTATION

2.3.1 Gages. Earth stress measurements were made with 1/4- and 1/2-inch-diameter tourmaline gages purchased from Crystal Research, Inc., Cambridge, Massachusetts. The 1/2-inch gages were employed in the predicted stress region from 2,500 psi to 3,500 psi, and the 1/4-inch gages for pressures higher than 3,500 psi. These gages had been used successfully in previous tests in the Pre-GONDOLA series[1].

Velocity gages used in this study were Sandia Model DX gages purchased from Spartan Industries, Albuquerque, New Mexico. These gages operate on the principle of the overdamped accelerometer. A variable reluctance sensor is used. A more detailed gage description can be found in Reference 1. Vertical particle velocity gages used were horizontal gages modified by the addition of a spring to counteract gravitational forces on the pendulum.

Accelerometers used were of two types: strain gage and variable reluctance. The accelerometer designated "200 AR CL" was a 1,000-G-capacity instrument made by Consolidated Electrodynamics Corporation, Pasadena, California, and that designated "150 AR CS" was made by Endevco Corporation, Pasadena, California. The remaining gages were variable reluctance type made by Pace Engineering Company, North Hollywood, California.

2.3.2 Gage Installation. A horizontal and a vertical velocity gage were mounted in a 5-1/2-inch-diameter canister with associated calibration electronics. The canister assembly was filled with paraffin for waterproofing and shockproofing of the contents. The electrical cable was fed to the ground surface through a 3/4-inch-diameter aluminum pipe threaded into the canister lid. The pipe also served as a placement and orientation device.

Signal cable from the tourmaline stress gages was protected with 1-inch rigid plastic pipe to the ground surface. The gage protruded 1 inch below the end of the plastic pipe. For installation the stress gage assembly was taped to the velocity gage canister so that it extended 6 inches below the bottom of the canister.

All main gage line instrument holes were deeper than

required gage depths and contained water to within a few feet of the surface. These were filled with sand to approximately 1 foot below the desired gage depth. This was accomplished by shoveling sand into the hole and allowing it to settle through the water. The entire gage assembly was then lowered to the desired depth and oriented. Sufficient sand was shoveled into the hole to ensure that the tourmaline pressure gage and part of the canister were surrounded by sand. A grout mix was then placed by 1-inch-diameter tremie pipe from the top of the sand forming a 3-foot-long plug. When the grout had set, the remainder of the hole was backfilled with sand.

Horizontal and vertical accelerometers were mounted in a 3-1/2- by 3-1/2- by 6-inch aluminum box which was filled with paraffin. The box was fastened to a 4- by 4-inch wood post that had been buried in the crater wall.

Electrical signals from the velocity gages and the two variable reluctance accelerometers located in the Charlie crater were carried on four-conductor shielded cable to a junction box (Figure 2.1) located approximately 500 feet from the charge row. Connections between the junction box and the WES instrumentation van were made with a 50-pair telephone cable. The two strain gage accelerometers required individual shielded cables and were not connected to the junction box.

Four-conductor shielded cable was used for all gages in the Delta crater.

Piezoelectric gage signals were carried on coaxial cable. A piece of "low noise" cable, approximately 100 feet long, was used at the gage. The remaining cable was standard coaxial. The low noise cable was utilized to prevent cable noise from obscuring the portion of the pressure-time history of interest. It was not necessary to bury any surface cable runs since the data of interest would have been retrieved before damage from crater ejecta.

2.3.3 Recording Systems. All instrumentation outputs, except from the tourmaline stress gages and strain gage accelerometers, were recorded on light-beam galvanometer oscillographs. The high-frequency outputs of the tourmaline stress gages and strain gage type accelerometers were recorded on an FM magnetic tape recorder. Signal conditioning equipment varied with the type of instrument; velocity gages and variable reluctance type accelerometers used a 3 kcps carrier-demodulator system; strain gage type accelerometers used a solid-state DC operational amplifier system; and the tourmaline stress gage used a cathode follower system.

All electronic recording equipment was housed in the WES recording van located approximately 2,100 feet south of the Pre-GONDOLA II row charge.

TABLE 2.1 MAIN GAGE LINE: GAGE TYPE AND SET RANGES

Gage No.	Gage Horizontal Distance from Charge	Gage Depth	Placement Hole No.	Gage Type	Predicted Peak
	ft	ft			
100 S 10	100	11.5	WES-1	Stress - Tourmaline	15,000 psi
100 UV 10	100	10.5	WES-1	Vertical Velocity	49 fps
100 UR 10	100	10.5	WES-1	Radial Velocity	130 fps
100 S 50	100	50.3	II-6	Stress - Tourmaline	18,000 psi
100 UV 50	100	49.3	II-6	Vertical Velocity	52 fps
100 UR 50	100	49.3	II-6	Radial Velocity	160 fps
150 S 10	150	11.5	WES-2	Stress - Tourmaline	8,700 psi
150 UV 10	150	10.5	WES-2	Vertical Velocity	26 fps
150 UR 10	150	10.5	WES-2	Radial Velocity	78 fps
150 S 50	150	50.3	II-7	Stress - Tourmaline	9,100 psi
150 UV 50	150	49.3	II-7	Vertical Velocity	28 fps
150 UR 50	150	49.3	II-7	Radial Velocity	86 fps
200 S 10	200	10.7	WES-3	Stress- Tourmaline	5,400 psi
200 UV 10	200	9.7	WES-3	Vertical Velocity	18 fps
200 UR 10	200	9.7	WES-3	Radial Velocity	52 fps
200 S 50	200	50.5	II-8	Stress - Tourmaline	6,100 psi
200 UV 50	200	49.5	II-8	Vertical Velocity	18 fps
200 UR 50	200	49.5	II-8	Radial Velocity	54 fps
300 S 10	300	11.0	WES-4	Stress - Tourmaline	3,400 psi
300 UV 10	300	10.0	WES-4	Vertical Velocity	14 fps
300 UR 10	300	10.0	WES-4	Radial Velocity	35 fps
300 S 50	300	50.2	II-9	Stress - Tourmaline	4,200 psi
300 UR 50	300	49.2	II-9	Radial Velocity	28 fps
400 S 50	400	49.7	II-10	Stress - Tourmaline	2,600 psi
400 RU 50	400	48.7	II-10	Radial Velocity	28 fps

Note: Horizontal distances shown are to closest charge.

TABLE 2.2 ACCELEROMETER LOCATION AND SET RANGES

Gage No.	Gage Horizontal Distance from Charge	Location	Gage Type	Predicted Peak
	ft			
200 AV CL	200	Charlie Lip	Vertical Accelerometer	220 G
200 AR CL	200	Charlie Lip	Radial Accelerometer	640 G
150 AV CS	150	Charlie Slope	Vertical Accelerometer	400 G
150 AR CS	150	Charlie Slope	Radial Accelerometer	1100 G
380 AV DL	380	Delta Lip	Vertical Accelerometer	33 G
380 AR DL	380	Delta Lip	Radial Accelerometer	98 G
425 AV DS	425	Delta Slope	Vertical Accelerometer	22 G
425 AR DS	425	Delta Slope	Radial Accelerometer	65 G
2100 AV CP	2100	Control Point	Vertical Accelerometer	0.6 G
2100 AR CP	2100	Control Point	Radial Accelerometer	1.9 G

Note: Horizontal distances shown are to closest charge.

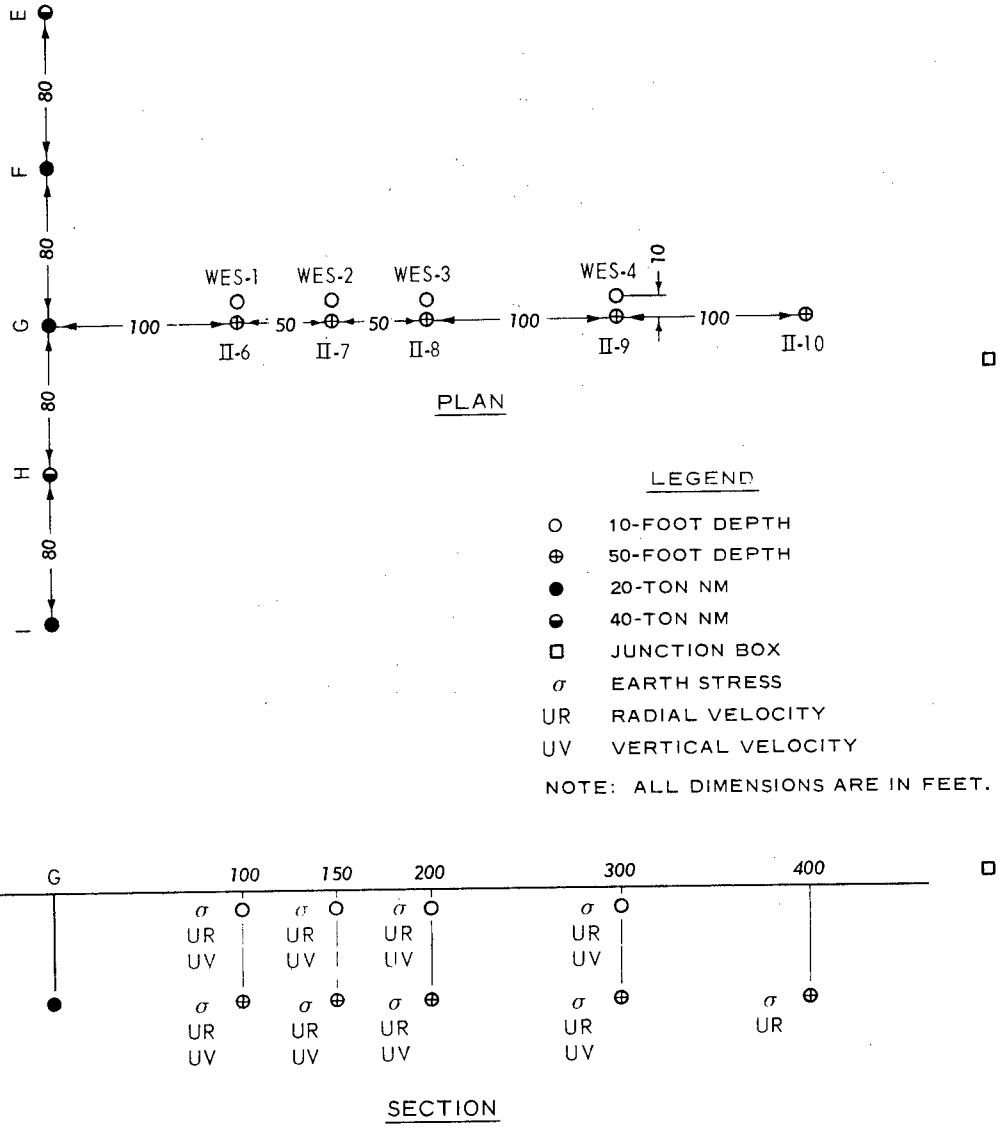

Figure 2.1 Layout of main gage line.

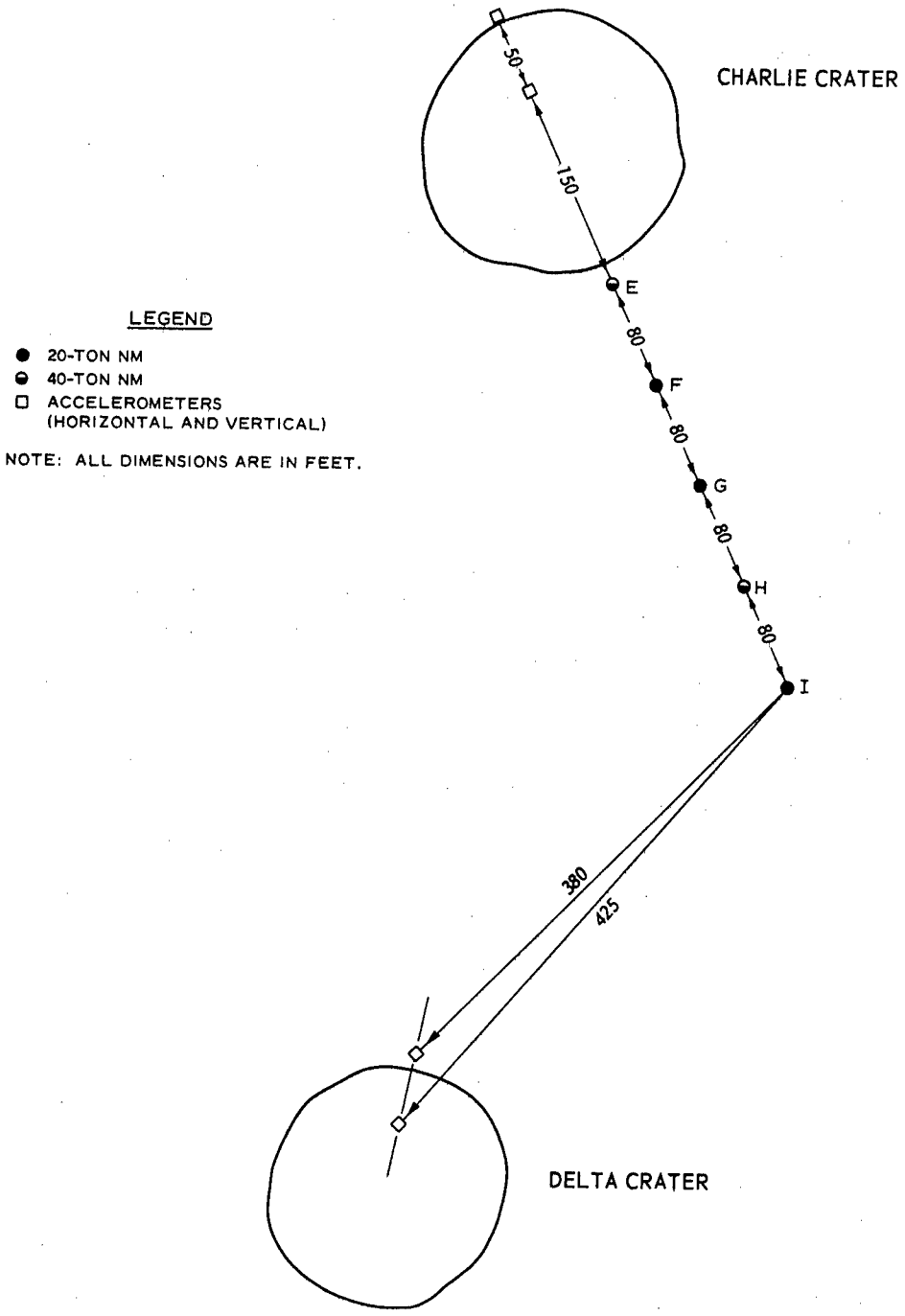

Figure 2.2 Accelerometer layout.

CHAPTER 3

RESULTS AND DISCUSSION

3.1 INSTRUMENT PERFORMANCE

All timing and sequence-initiating signals were received and properly translated, resulting in all recording equipment operating as planned.

Of the 35 gages installed for Pre-GONDOLA II, 32 were operable at shot time. Gage 100 S 50 apparently failed prior to detonation although resistance readings had given no indication of this condition. Equipment in the WES van sustained damage when the site transformer bank was hit by lightning, and lightning damage is suspected in the preshot failure of gage 200 AR CL, a strain gage accelerometer. After equipment repairs, a gage check revealed this gage to be inoperable. A resistance check, upon removal from the canister, showed all leads open. The cause of failure in 200 AV CL is not known. Three of the remaining gages (100 UV 10, 100 UV 50, and 200 UV 50) were overdriven and rendered only qualitative data.

3.2 DATA REDUCTION

The oscillograms and tape playbacks were read on an electro-mechanical digitizer, and the data converted to card form. These data cards were then processed through a digital computer where a temperature correction and an integration were performed

on the particle velocity records to yield displacements. All data were then automatically plotted.

Peak measurements of particle velocity and stress are summarized in Table 3.1. Acceleration peak values are presented in Table 3.2. Time histories of particle velocities and their associated displacements, soil stresses, and accelerations are presented in Appendix A.

3.3 ARRIVAL TIMES

Compressional wave front arrival times at all main line gages are plotted versus slant distance in Figure 3.1. The average propagation velocity based on gages at charge depth was 6,600 ft/sec. Gages at a nominal 10-foot depth yielded slightly longer arrival times and, consequently, a slower propagation velocity. The higher velocity at depth is probably due to more competent material at charge depth compared to the weathered zone near the surface.

The average compressional wave velocity (6,600 ft/sec) for the main gage line was lower than the value reported for the Pre-GONDOLA I[1] Bravo Event. The Pre-GONDOLA I value was based on gages spread over a greater distance. The shock wave traveled through deeper, more competent material to reach the farther gage stations. The result was a slightly higher velocity. The accelerometers located at the CP yielded a velocity comparable to the Pre-GONDOLA I value of 6,800 ft/sec.

More precise arrival times were obtained from the piezoelectric gage traces than from the particle velocity records because of the ability of the stress gages to respond faster.

3.4 SOIL STRESS

Initial peak stress versus slant distance is plotted in Figure 3.2. The 20-ton Pre-GONDOLA I[1] and scaled granite[4, 5] data are shown in this figure for comparison. The first disturbance sensed by all pressure gages in the main gage array was caused by charge G (with the exception of stations 300 and 400 feet from G, both at 50-foot depths). The compressional waves from charges F, G, and H coalesced after traveling approximately 290 feet and are not separately identifiable 300 feet from charge G. The compressional waves from charges E and I still lagged the coalesced wave slightly at the 400-foot station (see Figure A.12). Data from the deep gage stations 300 and 400 feet from G are presented at both actual (80 tons) and scaled distances (20 tons) in Figure 3.2. The scaling factor is $S = (W_1/W_2)^{1/3}$ where:

W_1 = combined charge weight (F, G, and H)

W_2 = charge weight being scaled (20 tons)

Initial peak stress data from the deep gages are consistently higher than those from shallow gages. The deep gages were located in stronger, saturated, more competent material which transmitted stronger shock. The shallow gages were apparently

located above the groundwater level which is estimated to be between 10 and 20 feet below ground surface in the Pre-GONDOLA II area[6]. In addition, wave forms recorded by shallow gages at stations 200 and 300 feet from charge G (gages 200 S 10 and 300 S 10, Figures A.6 and A.9) indicate the presence of an unloading or tensile (rarefaction) wave which further reduced peak values at these stations. The gage station 150 feet from charge G yielded initial peak stress data significantly higher than the general trend (gages 150 S 10 and 150 S 50, Figure A.3). That both deep and shallow gages responded in this manner indicates some cause other than gage error.

When a compressional wave impinges on a free surface or an interface of lower acoustical impedance, it is reflected as a tensile or unloading wave[7]. Tension is not recorded as such but is manifested as a decrease in compressive stress. When a gage is located in a medium with a sufficiently close boundary such that the difference between direct and reflected ray paths is small, tensile relief resulting in lower peak values can occur. The shallow gages were located close enough to the surface that tensile relief must be investigated. Consider the following:

	Gage			
	100 S 10 (Figure A.1)	150 S 10 (Figure A.3)	200 S 10 (Figure A.6)	300 S 10 (Figure A.9)
Computed Δ T (reflected-direct)	1.5 msec	1.4 msec	0.7 msec	0.3 msec
Apparent rise time (first peak)	0.3 msec	0.9 msec	0.5 msec	0.9 msec

The shock wave from a spherical source emanating into a homogeneous, continuous media, such as Bearpaw clay-shale, disperses and attenuates[7]. This causes a rounding of the shock front, resulting in longer rise times with distance. The comparison presented earlier shows a rise time increase with distance out to the 150-foot station (gage 150 S 10) while a shorter apparent rise time was measured at the 200-foot station (gage 200 S 10). The computed difference between reflected and direct arrival times at the 200-foot station is very close to the apparent rise time value, making tensile relief at this station a distinct possibility. A similar comparison at the 300-foot station (gage 300 S 10) indicates that tensile relief had taken place, resulting in a lower initial peak stress value.

Peak soil stress data are plotted versus slant distance in Figure 3.3. One gage (100 S 10) was damaged after recording the initial peak stress, resulting in loss of additional stress data from this gage. The deep gages recorded higher peak values than the shallow gages. This was partially due

to the stronger, saturated, more competent material found at depth but primarily was the result of the gage-charge geometry used for the shallow gages. Placement of these gages 10 feet north of the main gage line resulted in longer travel times for the stronger compressional wave from charge H (40 tons) than for charge F (20 tons). This difference decreases at greater distances. It is particularly evident when comparing deep and shallow gage data at the 150-foot station (gages 150 S 10 and 150 S 50, Figure A.3) as follows:

Charge		Gage 150 S 10		Gage 150 S 50	
No.	Weight, tons	Slant distance, feet	Travel time, msec	Slant distance, feet	Travel time, msec
G	20	155	24.1	150	21.9
F	20	170	25.6	170	24.4
H	40	182	26.4	170	24.4

The wave form at the deep 150-foot station (gage 150 S 50) shows that, as expected, the charge F and H compressional waves arrived almost simultaneously but the charge H compressional wave lagged the F wave by almost 1 msec at the shallow gage (150 S 10). This results in three distinct peaks (compressional waves from F, G, and H) with only a small increase in total peak stress at the shallow gage.

Examination of time-histories from the deep gages (Figures A.3, A.6, A.9, and A.12) indicates that the gaged area is in a transition zone. Peak stress at the 150-foot station (Figure A.3) is the sum of a partially decayed pulse from a 20-ton charge (G) and the contribution of a 40-ton (H) and a 20-ton (F) charge. As the distance increased, these compressional waves tended to coalesce. The wave form recorded at the 400-foot station (gage 400 S 50) indicates that charges F, G, and H have coalesced and input from charges E and I still lagged slightly.

The initial peak pressure attenuated as the -2 power of distance as was found for the Pre-GONDOLA I series. Total peak stress also attenuated as the -2 power of distance at the 300- and 400-foot stations. It must be noted that the effective input continually changed over the gaged region due to coalescence of shock waves from the separate charges. Although the compressional waves from all five charges had not coalesced at the 400-foot station it is probable that after coalescence attenuation would continue as the -2 power of distance.

3.5 PARTICLE VELOCITY

Initial horizontal particle velocity data are presented in Figure 3.4. Here (as with the stress measurements) the

initial peak values are inputs from charge G (20 tons) except the deep gages (300 UR 50 and 400 UR 50) at stations 300 and 400 feet from G. Data from these gages are presented in Figure 3.4 at both actual and scaled distances. An effective charge weight of 80 tons was assumed for scaling. Wave forms recorded by the shallow gages (200 UR 10 and 300 UR 10) at stations 200 and 300 feet from G indicate that tensile relief has taken place. In addition, the shallow gage at 200 feet from G was tilted with the arrival of the initial compressional wave and registered a higher than normal peak value. This data point is questionable.

Pre-GONDOLA I data (horizontal particle velocity) are included in Figure 3.4 for comparison. These data were not corrected for temperature in the original report[1]. The gage calibration procedure was performed at 65 F. Assuming the same ground temperature as at Pre-GONDOLA II (50 F), a temperature correction factor of 1.18 is applied. The three closest Pre-GONDOLA I measurements are indicated as low in Reference 1. The gage located at a slant distance of 97 feet was overdriven, while those at slant distances of 100 and 133 feet experienced tensile relief. The remaining Pre-GONDOLA I data points compare well within the usual data scatter (i.e. 20 percent) with the Pre-GONDOLA II data.

Vertical particle velocity data are presented in Figure 3.5, and exhibit considerable scatter. Wave forms registered at the

shallow stations 200 and 300 feet from G (gages 200 UV 10 and 300 UV 10) indicate that there has been some tensile relief of peak values. The gage at the station 200 feet from G (gage 200 UV 10) also indicates early tilting, making the initial peak value questionable.

Particle velocity-time histories and first integrals (displacement) are presented in Appendix A. No base line corrections were applied to the velocity data. Therefore, the integral-time history (displacement), relative data at best, must be regarded as only qualitative.

3.6 ACCELERATION MEASUREMENTS

Peak acceleration data are plotted versus horizontal distance in Figure 3.6. In retrospect, the peak acceleration predictions were overly conservative. They were based on the assumption of competent material and did not take into account the presence of the intervening crater (in the case of measurements on the Charlie crater lip). Moreover, only empirical information was available preshot. The combination of these factors (effect of crater boundaries and rubble) strongly influenced the maximum surface accelerations at the close-in stations. However, estimates for the CP motions were much better, and excellent measurements were obtained at this location.

Based on arrival time data at Delta crater (gages 380 AR DL and 425 AV DS), a propagation velocity of 4,000 ft/sec was computed using the distance to the closest charge (I). This value is much slower than the 6,600 ft/sec value computed for the main gage line instrumentation. The discrepancy is explained as follows. Propagation velocity computations are an average value for all the material between two points, in this case between the closest charge (I) and the Delta crater gages. Two distinctly different materials are encountered by a shock wave traversing this line; crater rubble and a more competent clay-shale. Consider the gage located on the Delta crater slope (425 AV DS) with an arrival time of 106.6 msec. Assuming a propagation velocity of 6.6 ft/msec in clay-shale and 1.5 ft/msec in the rubble, a path approximately 80 feet long through the rubble would result in an average velocity of 4,000 ft/sec at this gage. Delta crater rupture zone measurements were not made. Excavation of the Bravo crater (also a single-charge 20-ton experiment in similar material) gave the following information*:

* PNE-1103, in preparation.

Radius from Charge, feet	Depth to Base of Rupture Zone, feet
125	60
175	43
225	21
375	0

Gage 425 AV DS was located approximately 10 feet below the original ground surface at a 50-foot radius from the center of the Delta crater. Based on the above information, an 80-foot-long path in rubble appears realistic.

The accelerometer (150 AV CS) located on the Charlie crater slope was situated on the far side of the crater away from the closest charge (E). The shock wave reaching the gage had to travel under or around the intervening crater through the rubble. This resulted in a longer compressive wave ray path to the gage and a higher average velocity than the 2,000 ft/sec computed using the horizontal gage-charge distance. Charlie crater is located at the edge of the Fort Peck Reservoir which had a pool elevation at Pre-GONDOLA II shot time of 2,243*[6]. This was 5 feet above the pool elevation at the end of the Pre-GONDOLA I series. The bottom of the Charlie crater is at elevation 2,220 which is 18 feet below the pool elevation at the end of Pre-GONDOLA I. Therefore, the rubble

* Elevations are in feet referred to mean sea level.

under the Charlie crater was probably saturated, which would result in higher average velocities at this location than at the Delta crater.

TABLE 3.1 PEAK MEASUREMENTS FROM VELOCITY AND STRESS GAGES (MAIN GAGE LINE)

No.	Horizontal Distance from Charge	Slant Distance from Charge	Depth	Arrival Time	Shock Wave				Remarks
					Initial Peak Value		Maximum Peak Value		
					Particle Velocity	Stress	Particle Velocity	Stress	
	ft	ft	ft	msec	ft/sec	psi	ft/sec	psi	
100 S 10	100	107	11.5	16.0		3,600			
100 UV 10	100	108	10.5	16.1					Gage overranged
100 UR 10	100	108	10.5	16.1	110		160		
100 S 50	100	100	50.3						Gage failed preshot
100 UV 50	100	100	49.3	14.2					
100 UR 50	100	100	49.3	14.2	280				
150 S 10	150	155	11.5	24.1		4,800		14,000	Peak value appears high
150 UV 10	150	155	10.5	24.1	24				
150 UR 10	150	155	10.5	24.1	73				
150 S 50	150	150	50.3	21.9		15,000		31,000	Peak value appears high
150 UV 50	150	150	49.3	22.4	4.5				
150 UR 50	150	150	49.3	22.5	32				
200 S 10	200	204	10.7	32.2		340		1,700	Tensile relieved
200 UV 10	200	204	9.7	34.4	4.2				Tensile relieved
200 UR 10	200	204	9.7	33.6	83				Tensile relieved
200 S 50	200	200	50.5	30.3		3,000		6,500	
200 UV 50	200	200	49.5	30.3					Gage overdriven
200 UR 50	200	200	49.5	30.5	37				
300 S 10	300	303	11.0	46.4		160		810	Tensile relieved
300 UV 10	300	303	10.0	48.7	12				Tensile relieved
300 UR 10	300	303	10.0	48.7	4.2				Tensile relieved

Note: Horizontal distances shown are to closest charge.

TABLE 3.1 PEAK MEASUREMENTS FROM VELOCITY AND STRESS GAGES (MAIN GAGE LINE) (continued)

Gage No.	Horizontal Distance from Charge	Slant Distance from Charge	Depth	Arrival Time	Shock Wave: Initial Peak Value Particle Velocity	Shock Wave: Initial Peak Value Stress	Shock Wave: Maximum Peak Value Particle Velocity	Shock Wave: Maximum Peak Value Stress	Remarks
	ft	ft	ft	msec	ft/sec	psi	ft/sec	psi	
300 S 50	300	300	50.2	45.0		4,700		4,700	
300 UR 50	300	300	49.2	46.4	29		29		
400 S 50	400	400	49.7	60.3		2,700		2,700	
400 UR 50	400	400	48.7	61.0	17		17		

NOTE: Velocities corrected for temperature
Vertical motion, positive = upward
Radial motion, positive = outward

Horizontal distances shown are to closest charge.

TABLE 3.2 PEAK MEASUREMENTS FROM ACCELEROMETERS

Gage No.	Gage Horizontal Distance from Charge	Gage Location	Shock Wave Arrival Time	Acceleration Initial Peak Value	Acceleration Maximum Peak Value	Remarks
	ft		msec	G	G	
200 AV CL	200	Charlie Crater Lip				Gage failed preshot
200 AR CL	200	Charlie Crater Lip				Gage failed preshot
150 AV CS	150	Charlie Crater Slope	80.2	20	20	
150 AR CS	150	Charlie Crater Slope		< 30	< 30	
380 AV DL	380	Delta Crater Lip		< 0.9	< 0.9	
380 AR DL	380	Delta Crater Lip	96.5	6.2	6.2	
425 AV DS	425	Delta Crater Slope	106.6	1.4	1.4	
425 AR DS	425	Delta Crater Slope		< 0.7	< 0.7	
2100 AV CP	2100	Control Point	307.8	0.94	1.3	
2100 AR CP	2100	Control Point	307.8	0.23	0.48	

NOTE: Vertical motion, positive = upward
Radial motion, positive = outward

Horizontal distances shown are to closest charge.

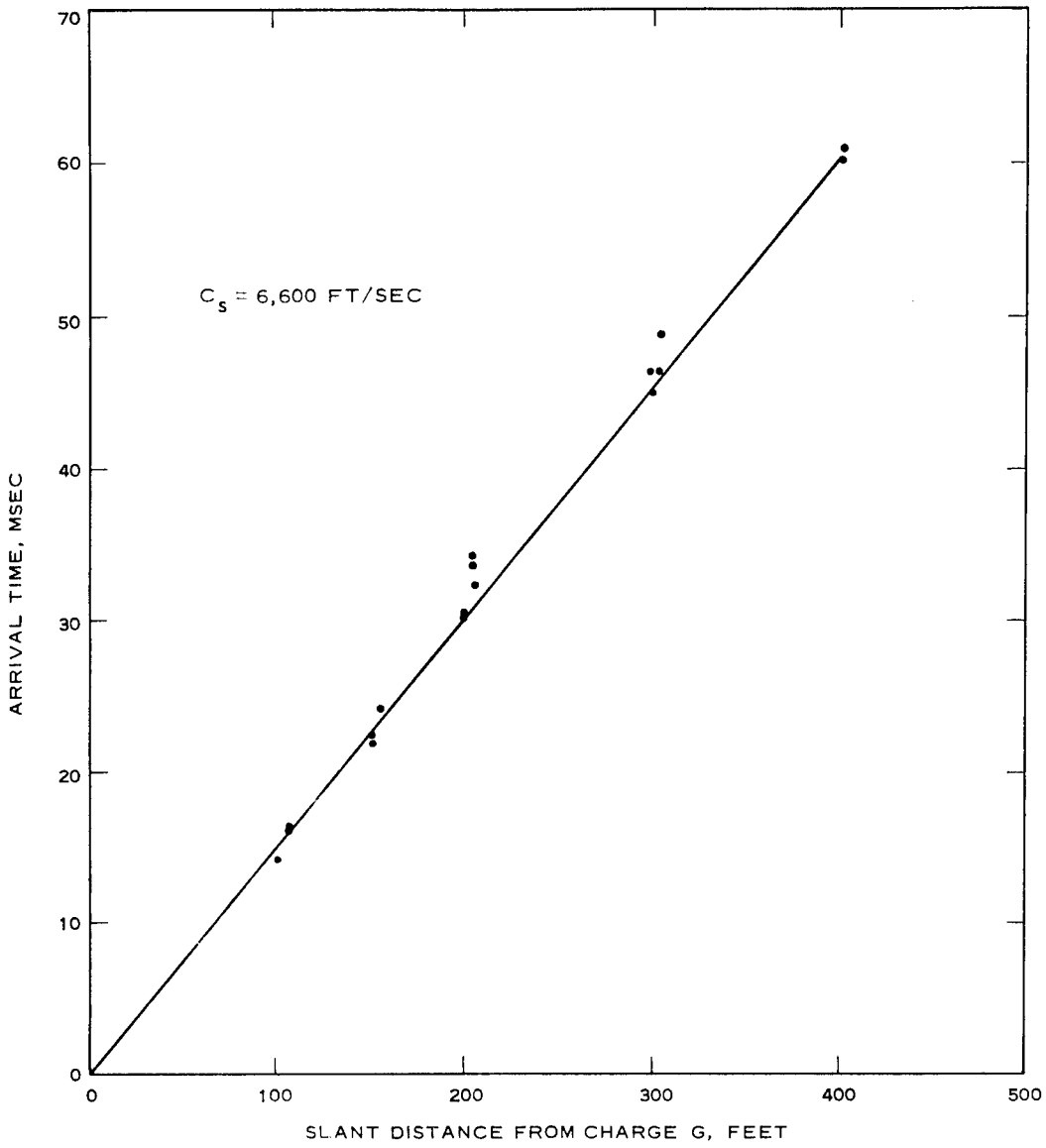

Figure 3.1 Arrival time versus distance.

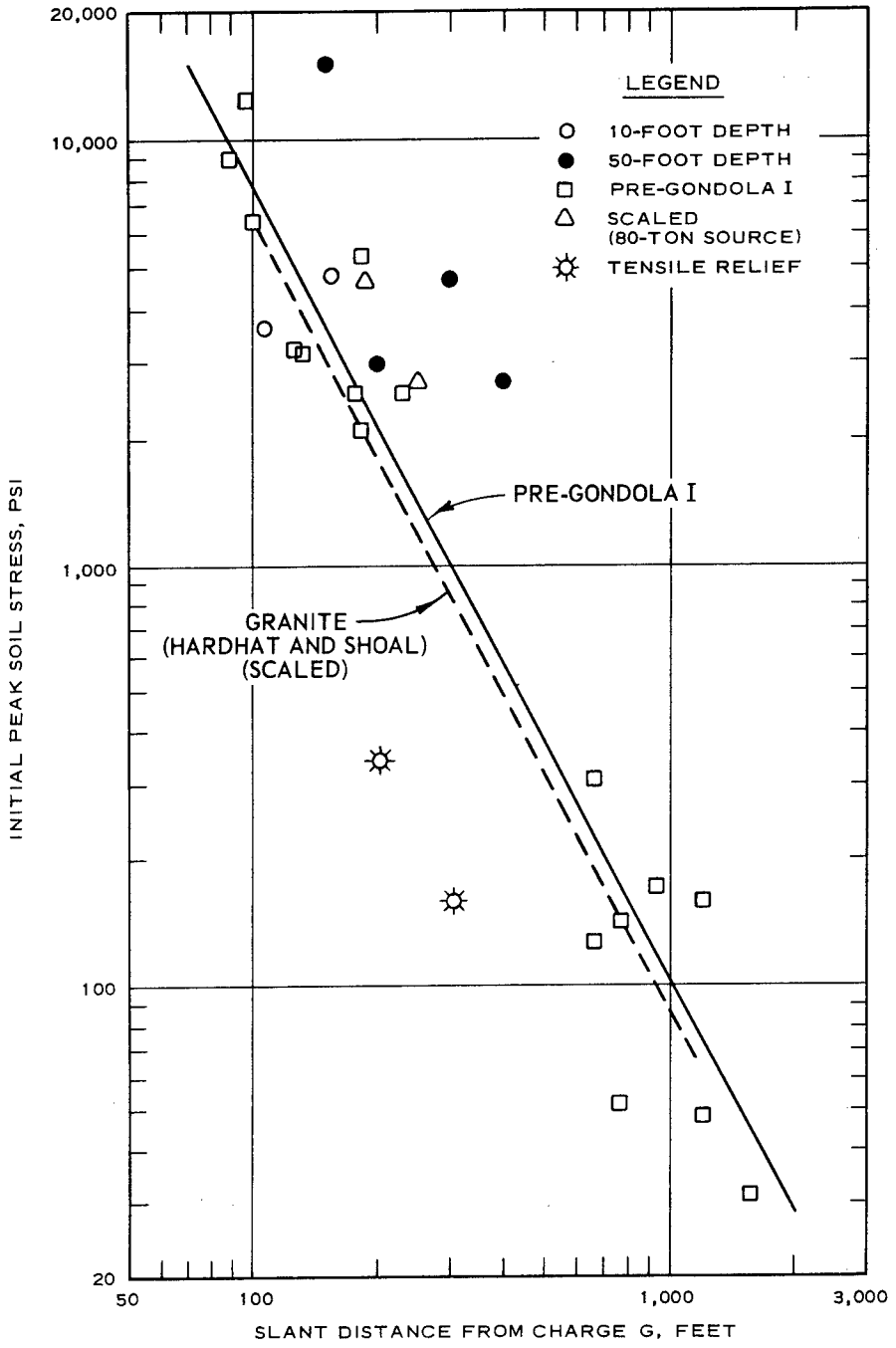

Figure 3.2 Initial peak soil stress versus slant distance.

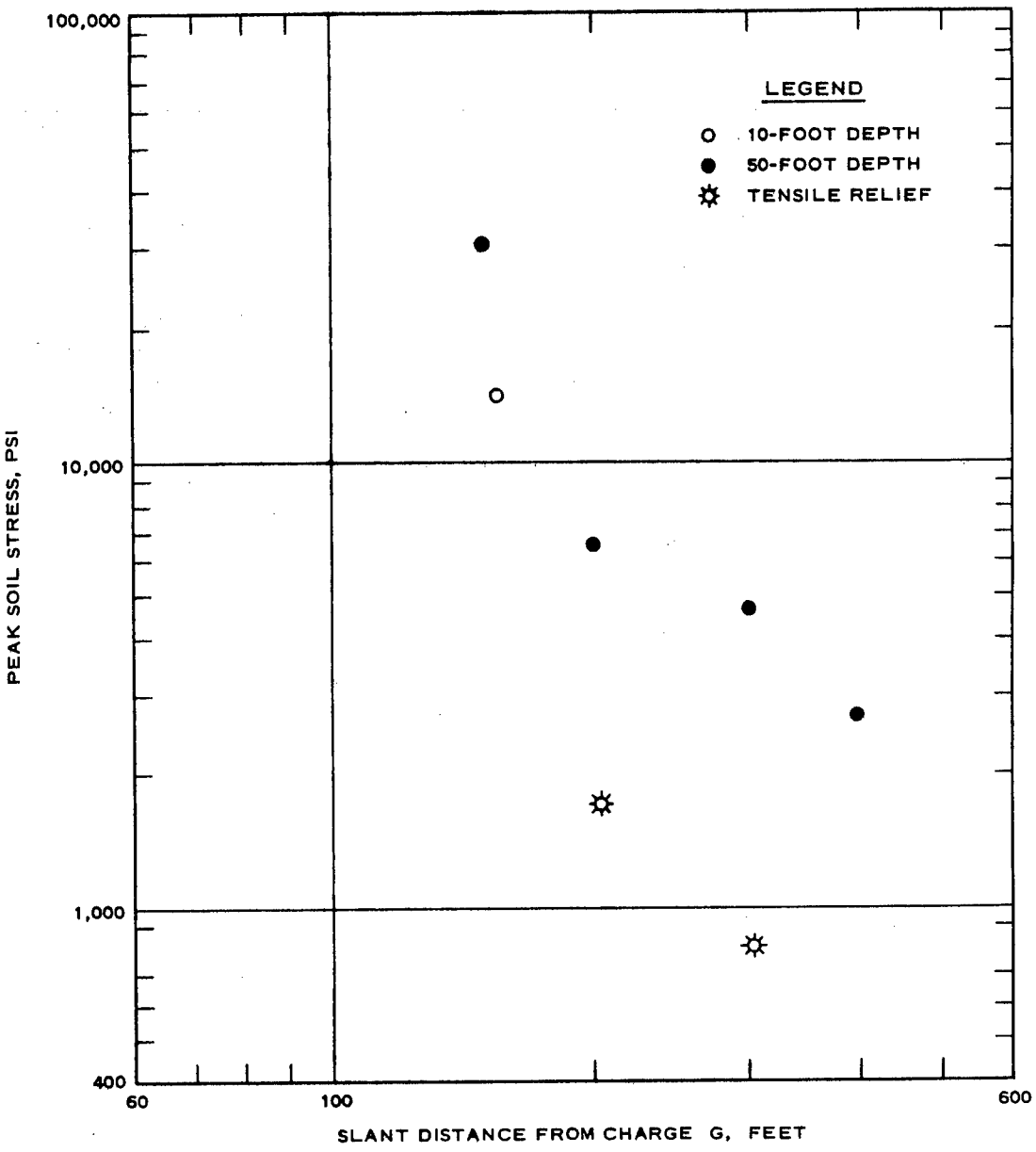

Figure 3.3 Peak soil stress versus distance.

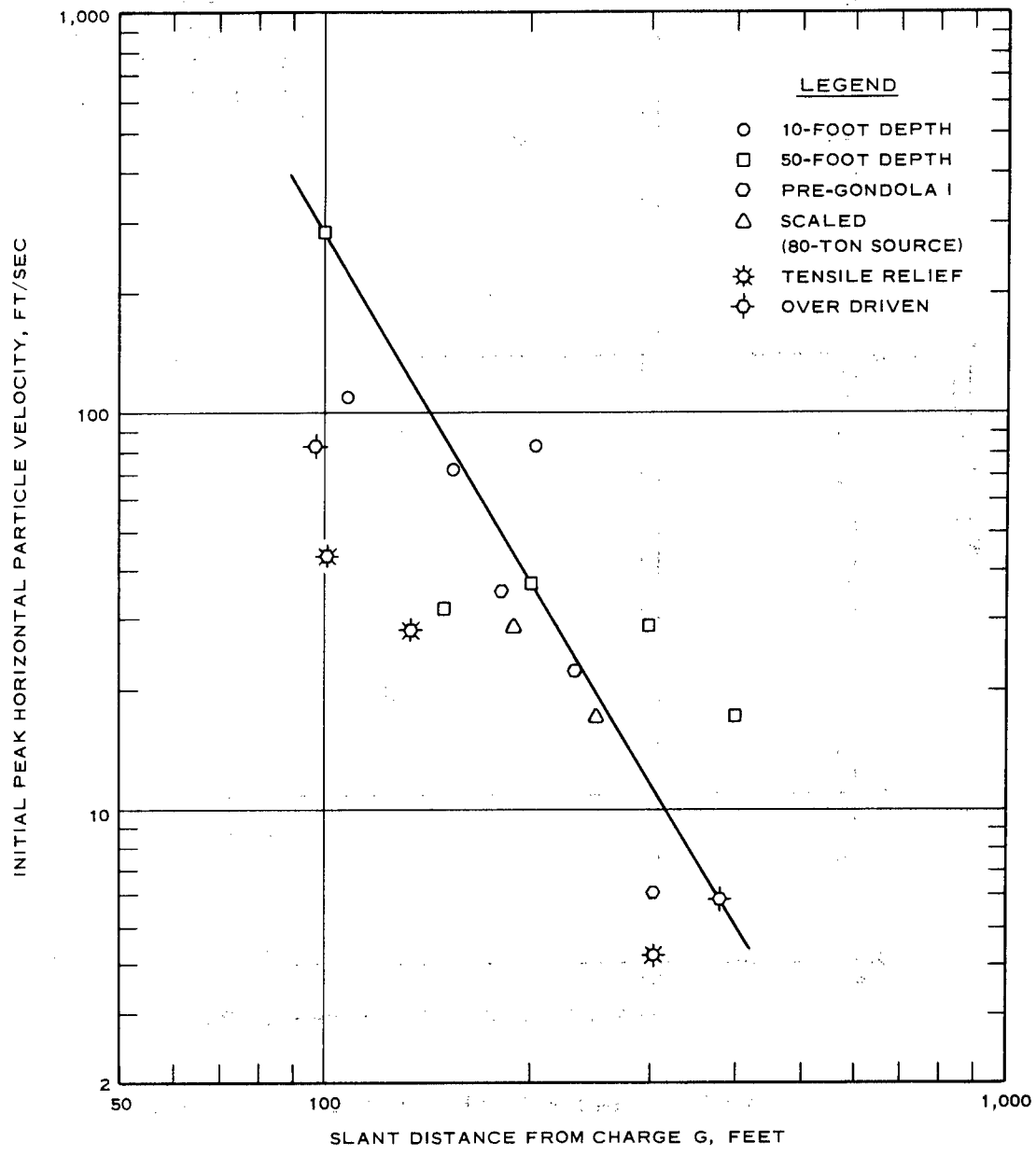

Figure 3.4 Initial peak horizontal particle velocity versus distance.

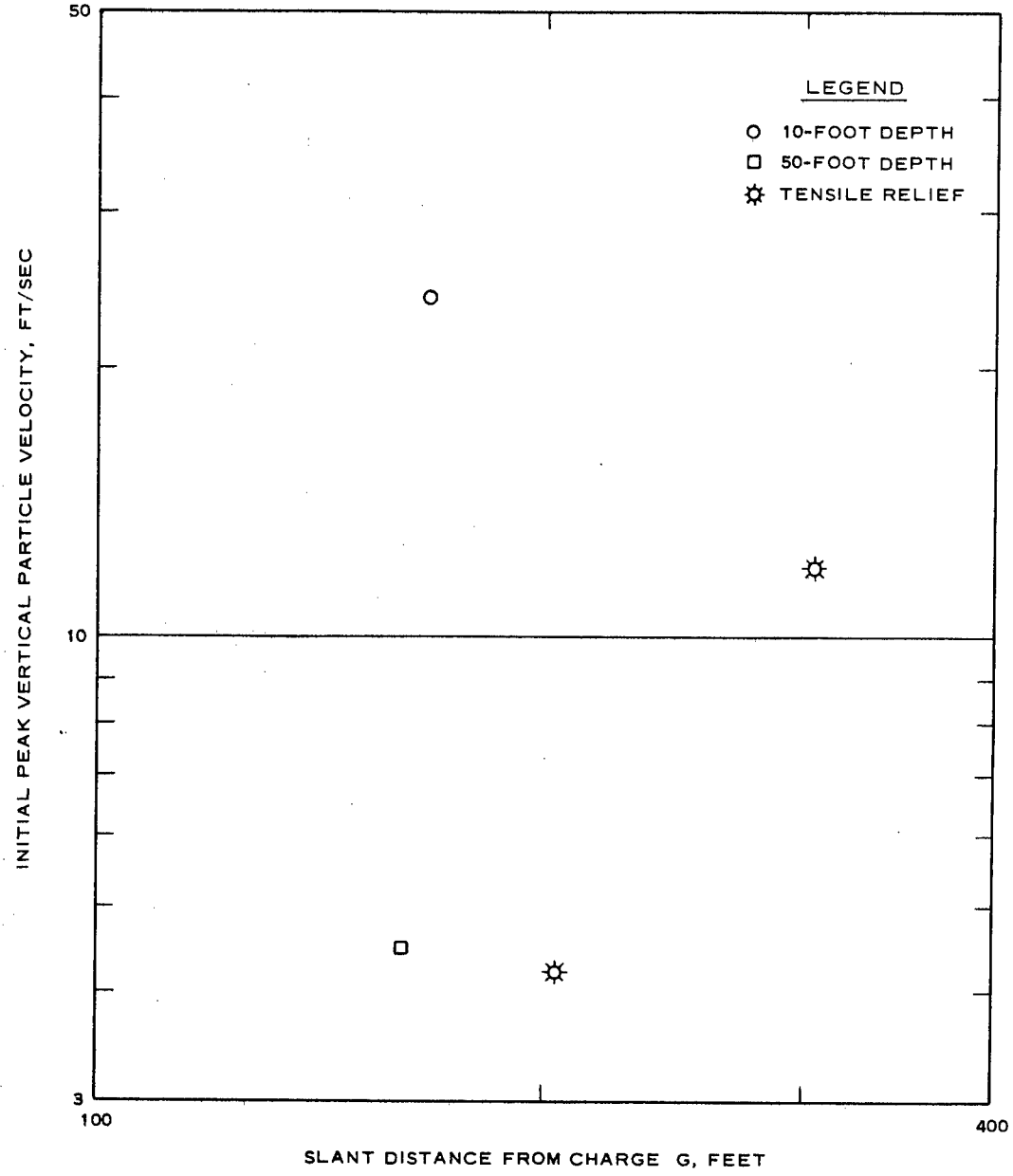

Figure 3.5 Initial peak vertical particle velocity versus distance.

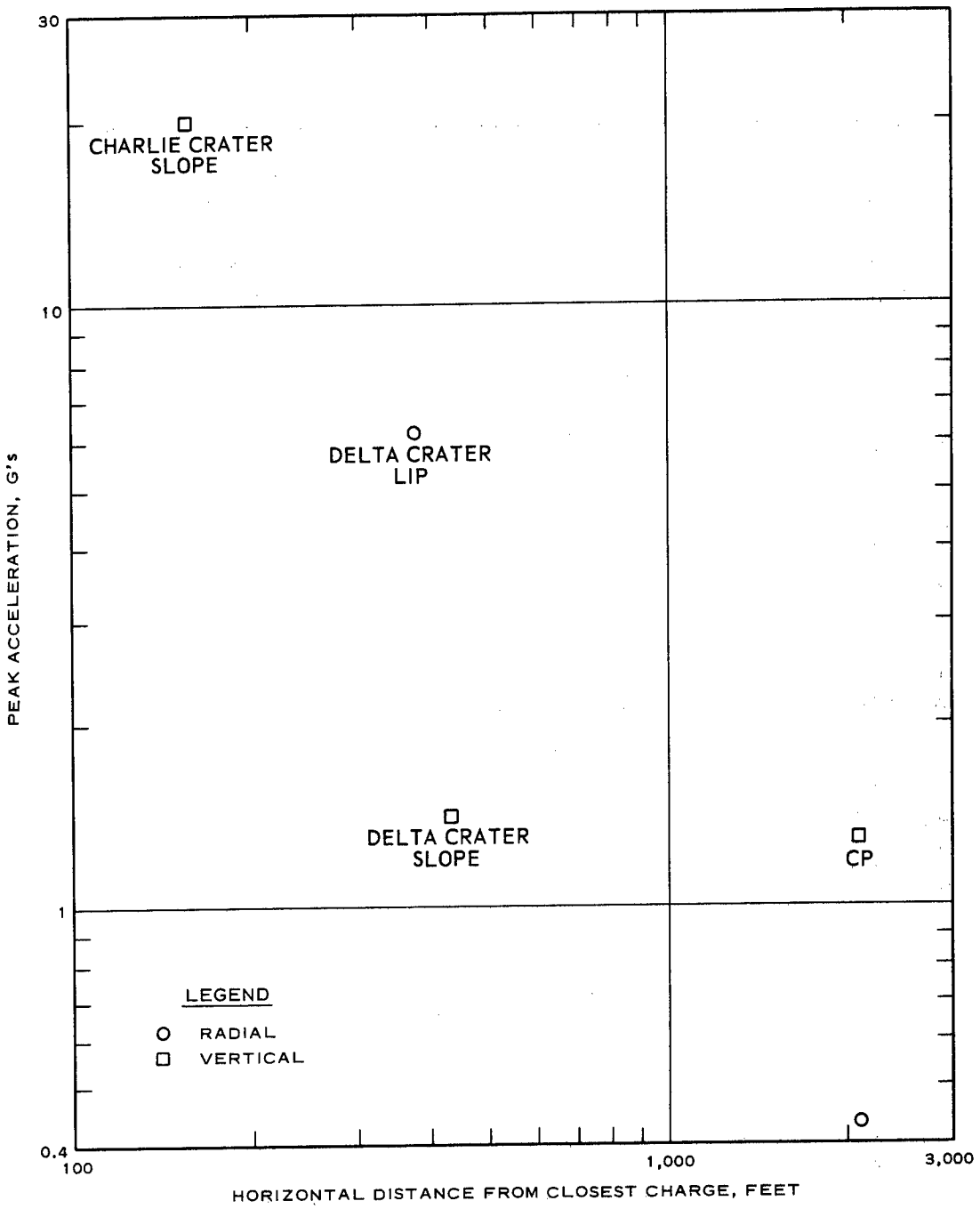

Figure 3.6 Peak acceleration versus distance.

CHAPTER 4

CONCLUSIONS

The computed Pre-GONDOLA II propagation velocity was 6,600 ft/sec. This is lower than the value reported for Pre-GONDOLA I. The Pre-GONDOLA I value is an average value over a longer distance. The shock wave reaching the farther gages travels through a deeper, more saturated, more competent, denser material.

Initial peak stress data are the result of input from charge G (20 tons) at all stations except the deep gages 300 and 400 feet from G. These exceptions scale using the combined charge weights of F, G, and H (80 tons). Wave forms indicate tensile cutoff of peak values at shallow stations 200 and 300 feet from G. Although higher initial stresses were measured from Pre-GONDOLA II than I, both attenuated as the -2 power of distance.

Peak stress measurements were obtained in a transition zone where the effective charge input was changing with distance. As the charge-to-gage distance increased, individual compressional waves began to coalesce, resulting in higher stresses with distance than found for initial peak data. Pulses from charges F, G, and H coalesced approximately 290 feet from charge G, but all five charge inputs had not coalesced at the 400-foot station. Placement of the shallow

gages 10 feet north of the main gage line resulted in a loss of symmetry. Thus, greater distances were required for the individual compressional waves to coalesce. Where coalescence is complete, scaling using combined charge weights of the coalesced pulse is effective.

Initial peak horizontal velocity similar to initial stress is the result of input from charge G (20 tons) at all stations except the deep gages 300 and 400 feet from G. Peak values at these stations scale using cube-root scaling and combined charge weights of F, G, and H (80 tons). These data compare well to Pre-GONDOLA I data.

Peak acceleration predictions for the crater slopes were based on competent material and did not take into account the presence of the intervening crater rupture zone. This method resulted in good predictions at the CP, but did not predict the low motions on the Charlie and Delta crater slopes. Maximum surface accelerations on the crater slopes were strongly influenced by the effects of crater boundaries and rubble.

APPENDIX A

STRESS-, ACCELERATION-, VELOCITY-, AND DISPLACEMENT-TIME HISTORIES

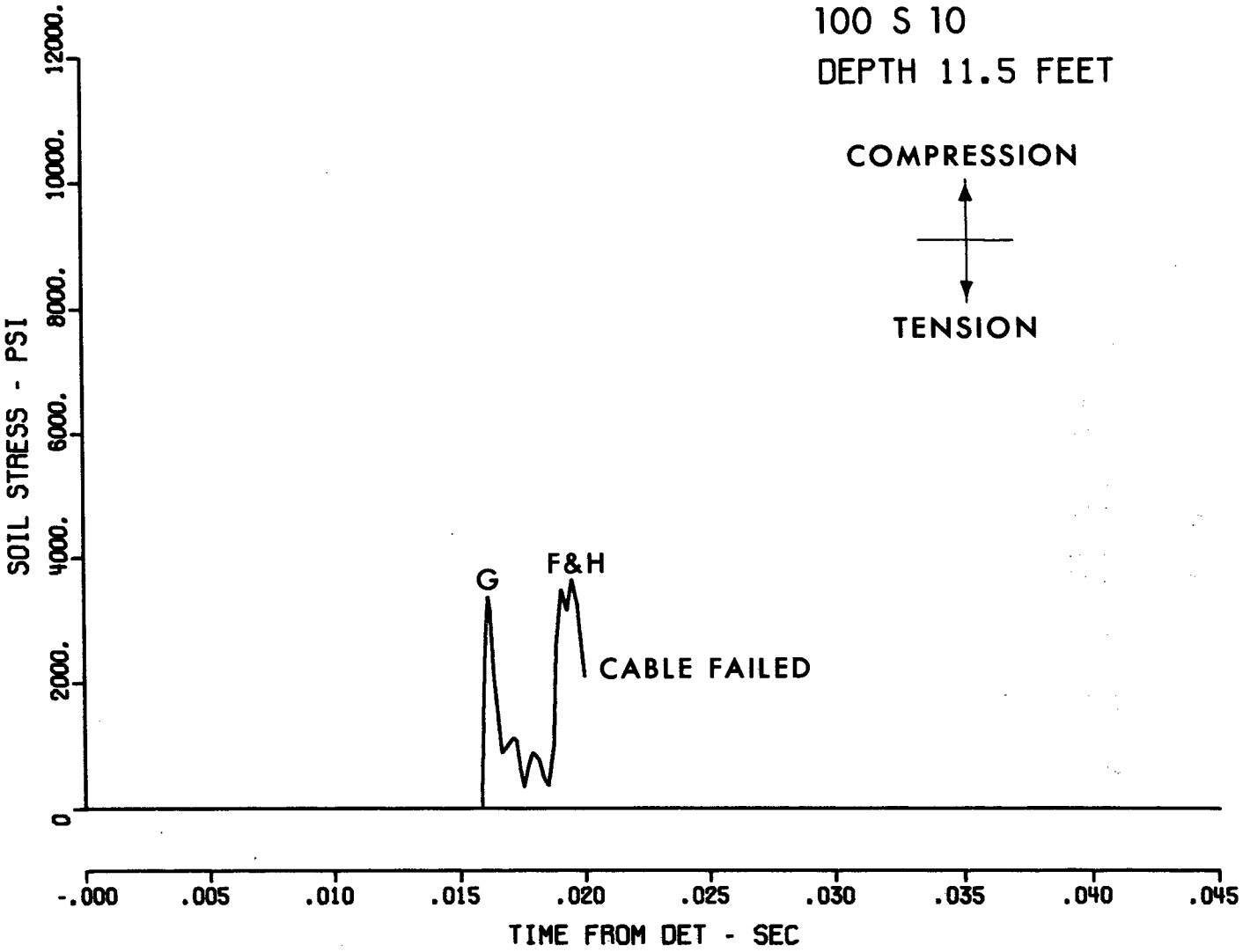

Figure A.1 Stress time history, Station 100

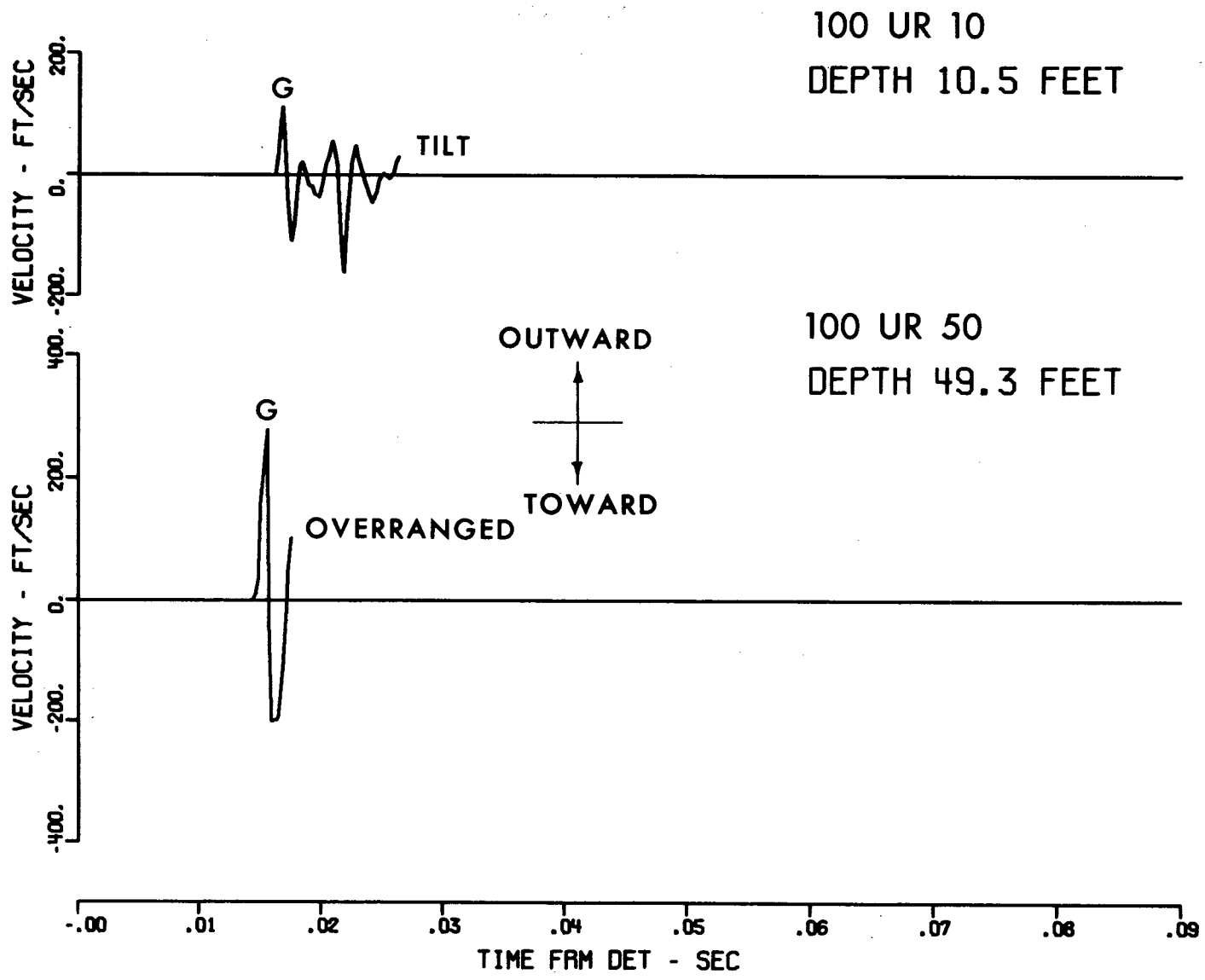

Figure A.2 Radial velocity time histories, Station 100

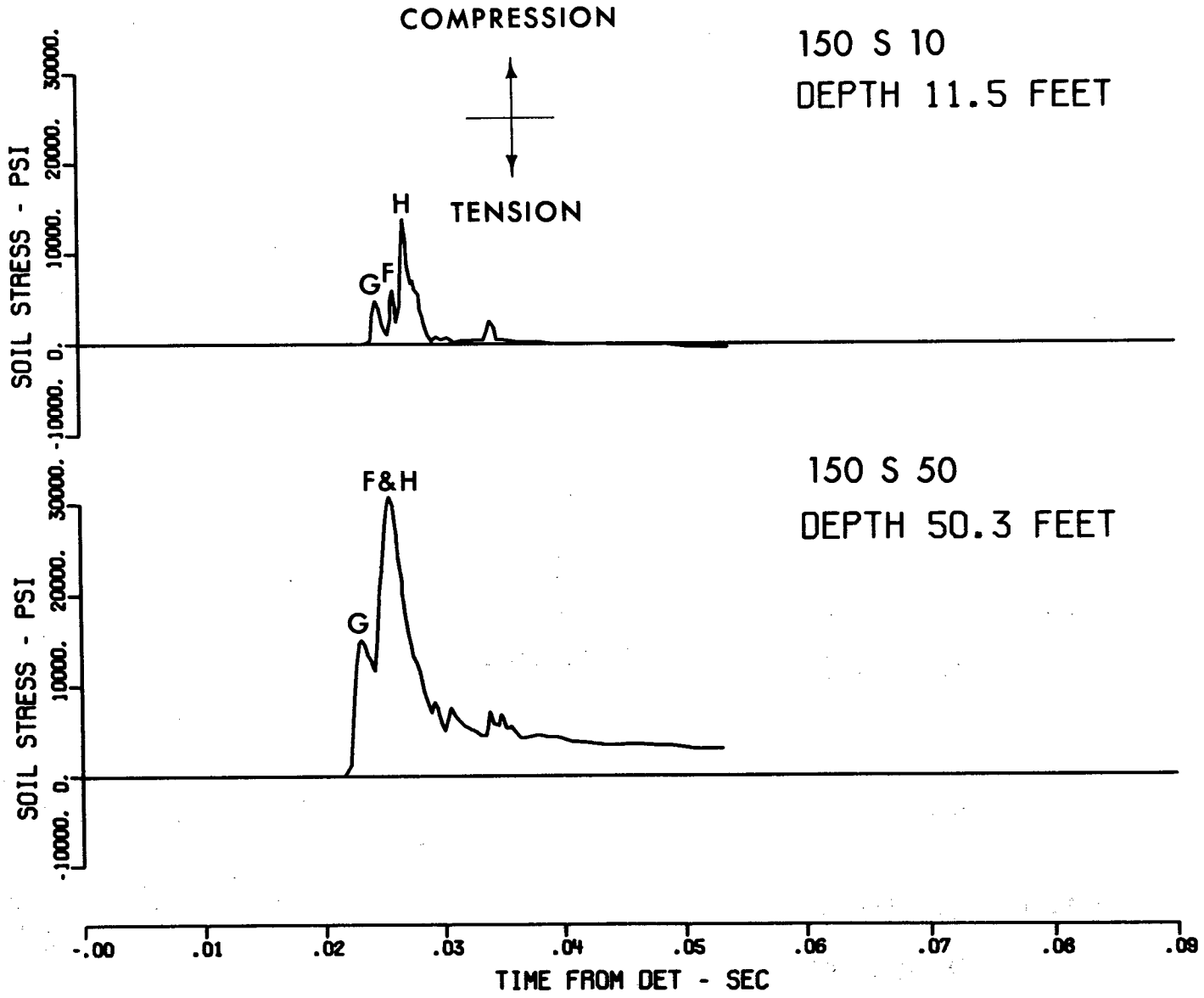

Figure A.3 Stress time histories, Station 150

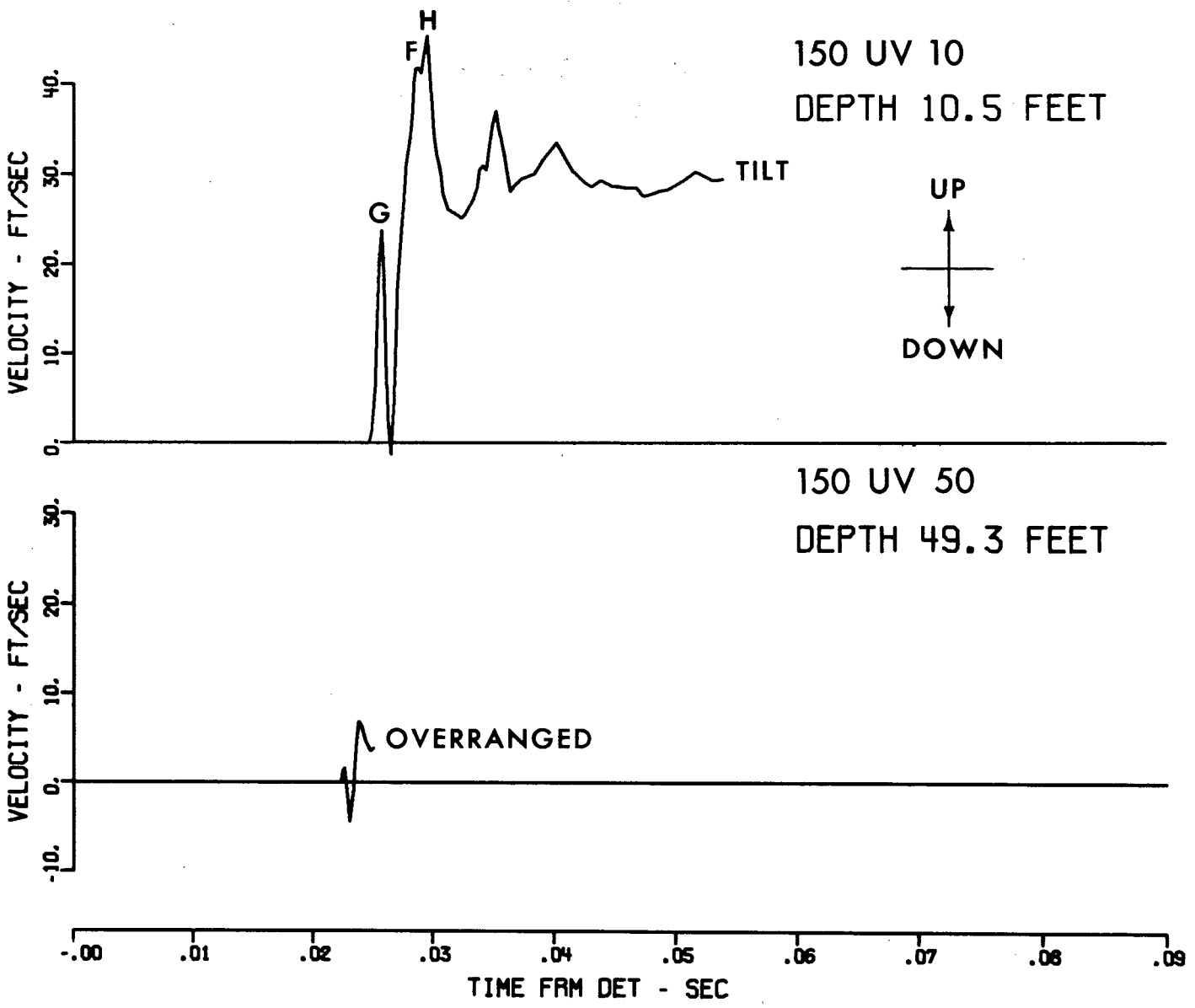

Figure A.4 Vertical velocity time histories, Station 150

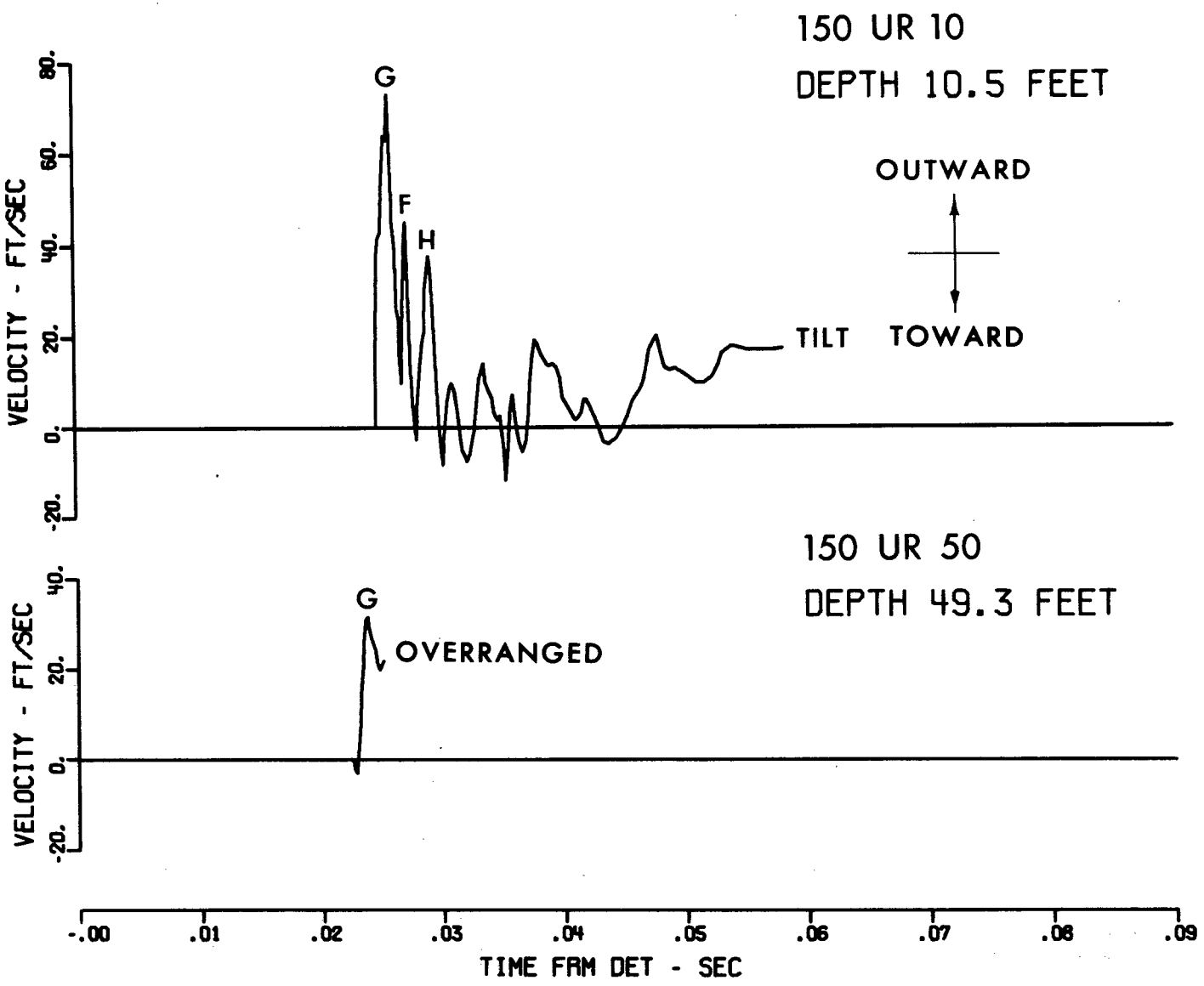

Figure A.5 Radial velocity time histories, Station 150

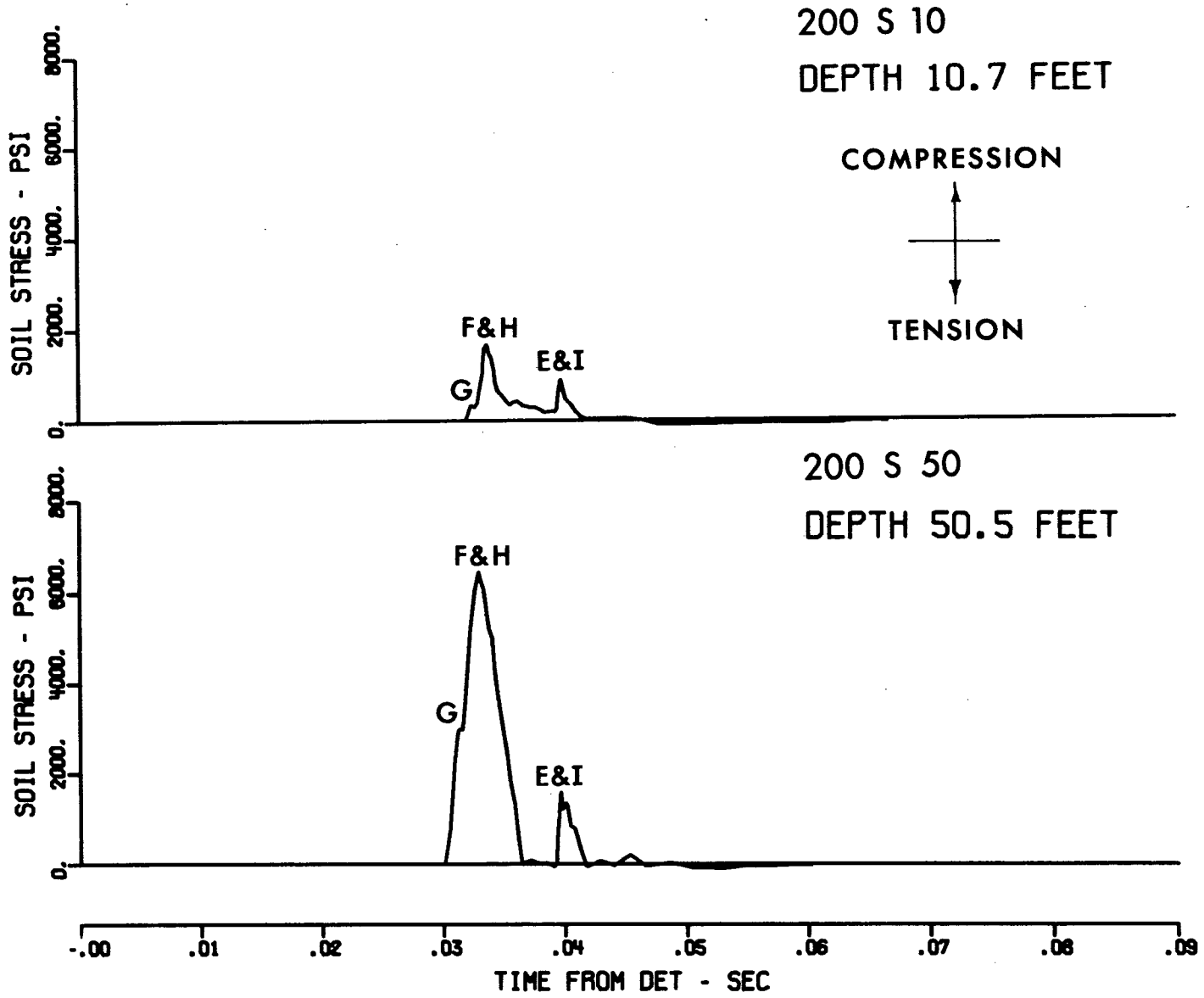

Figure A.6 Stress time histories, Station 200

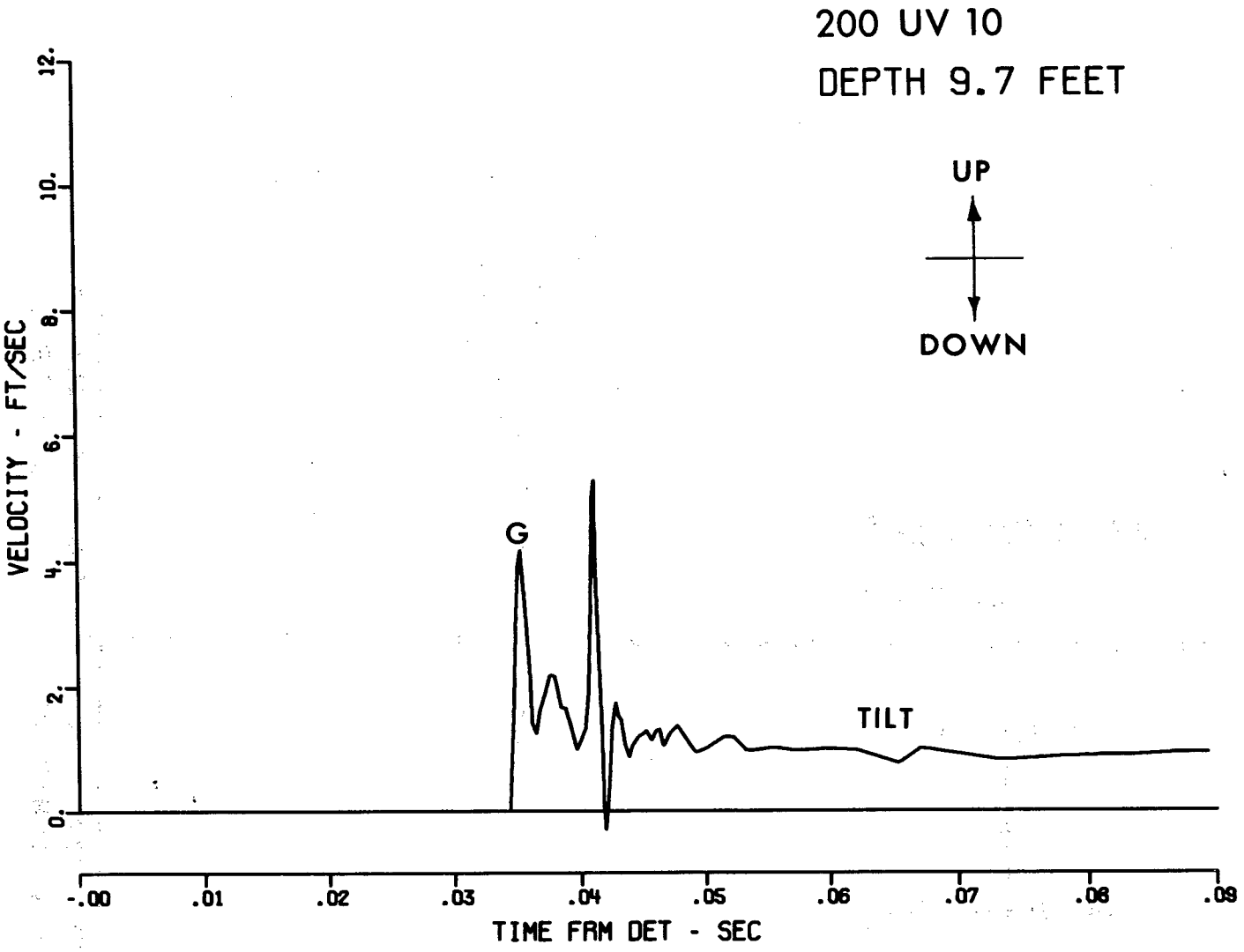

Figure A.7 Vertical velocity time history, Station 200

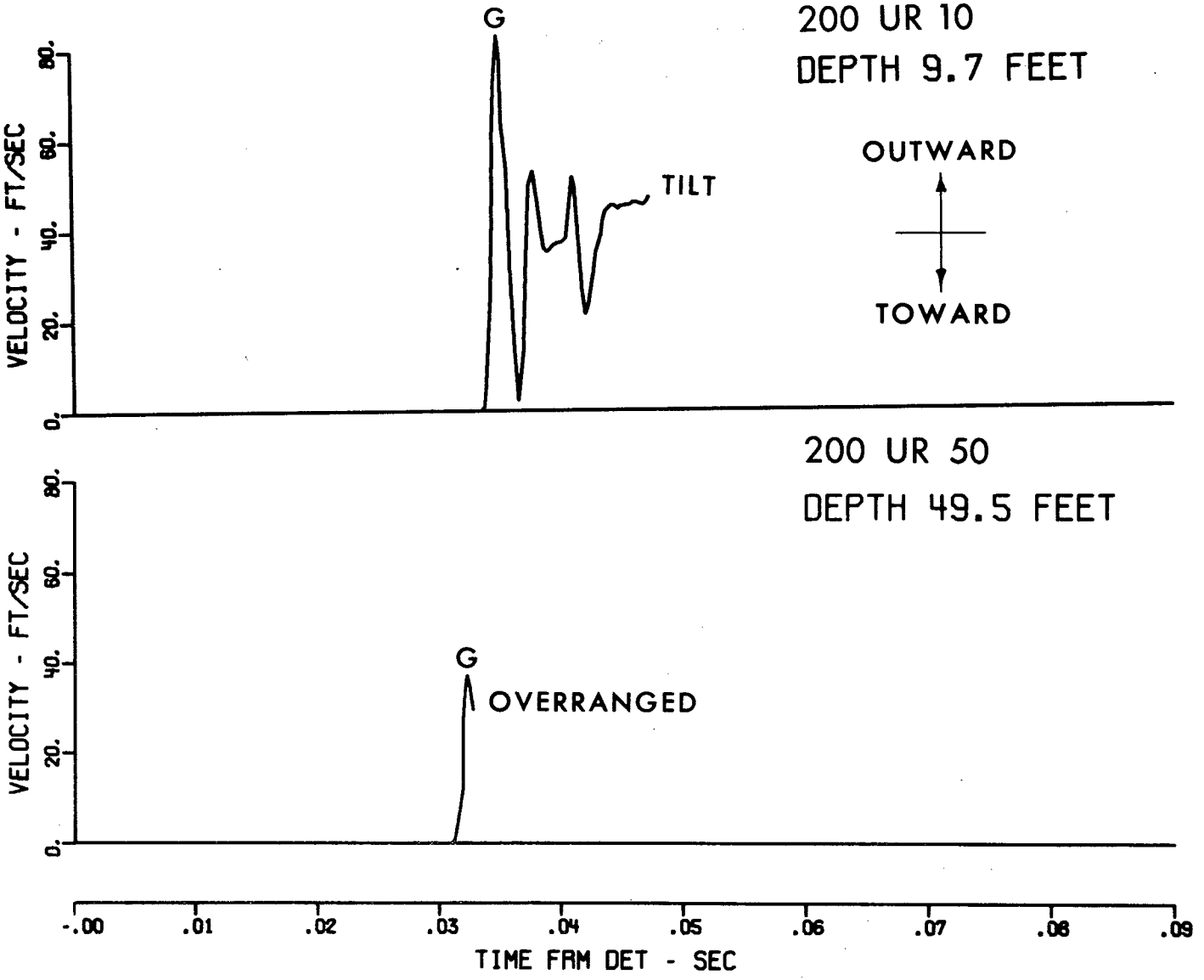

Figure A.8 Radial velocity time histories, Station 200

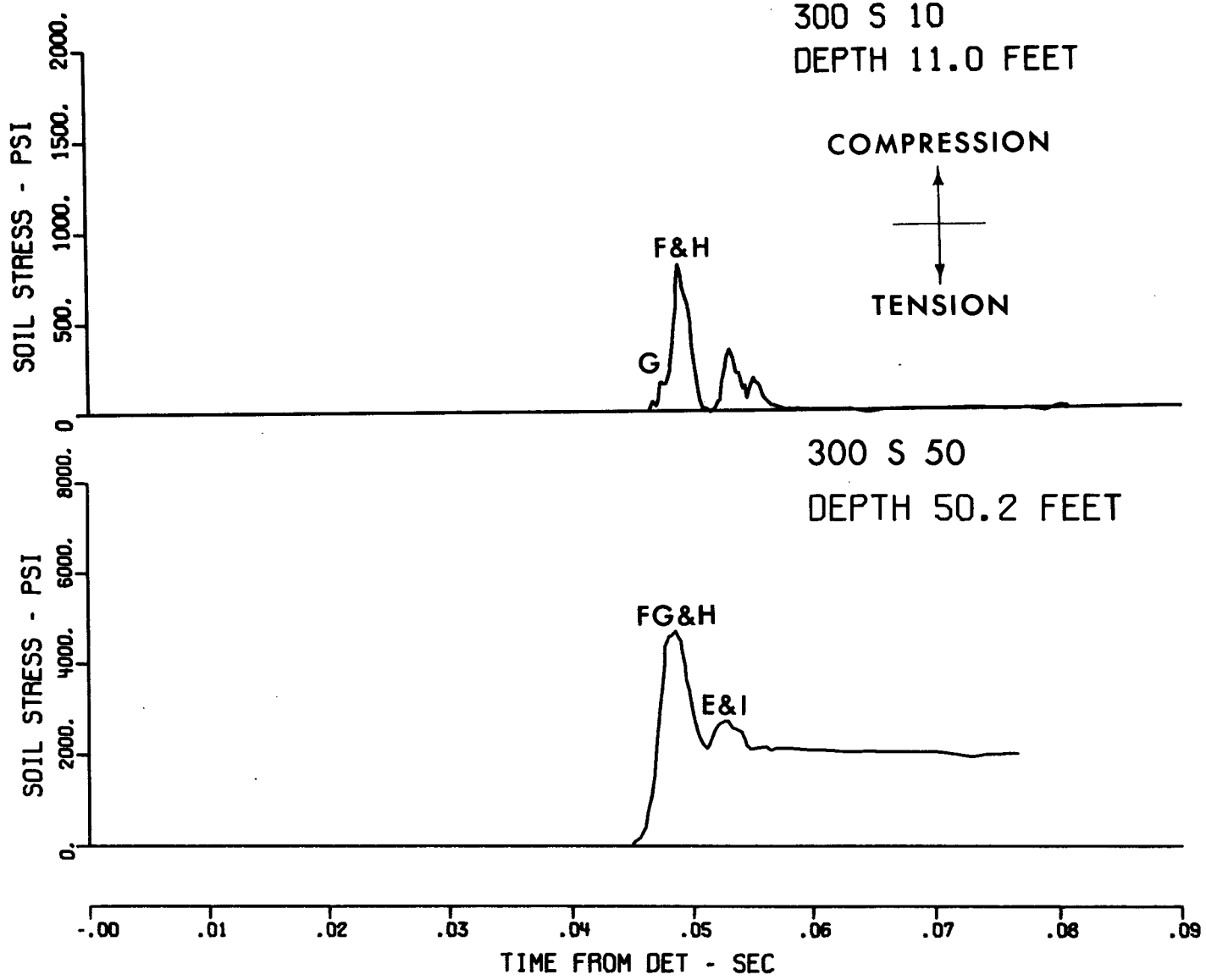

Figure A.9 Stress time histories, Station 300

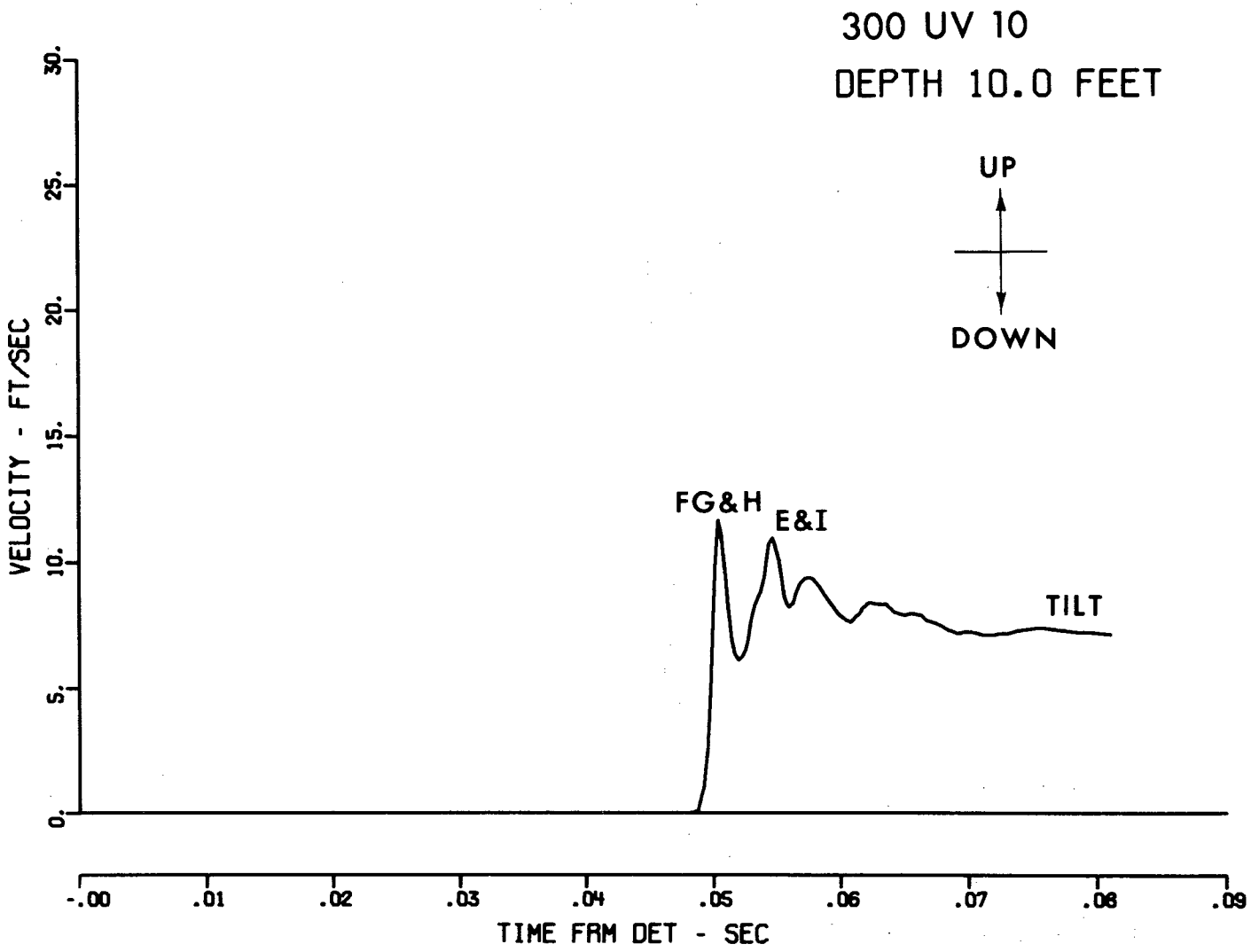

Figure A.10 Vertical velocity time history, Station 300

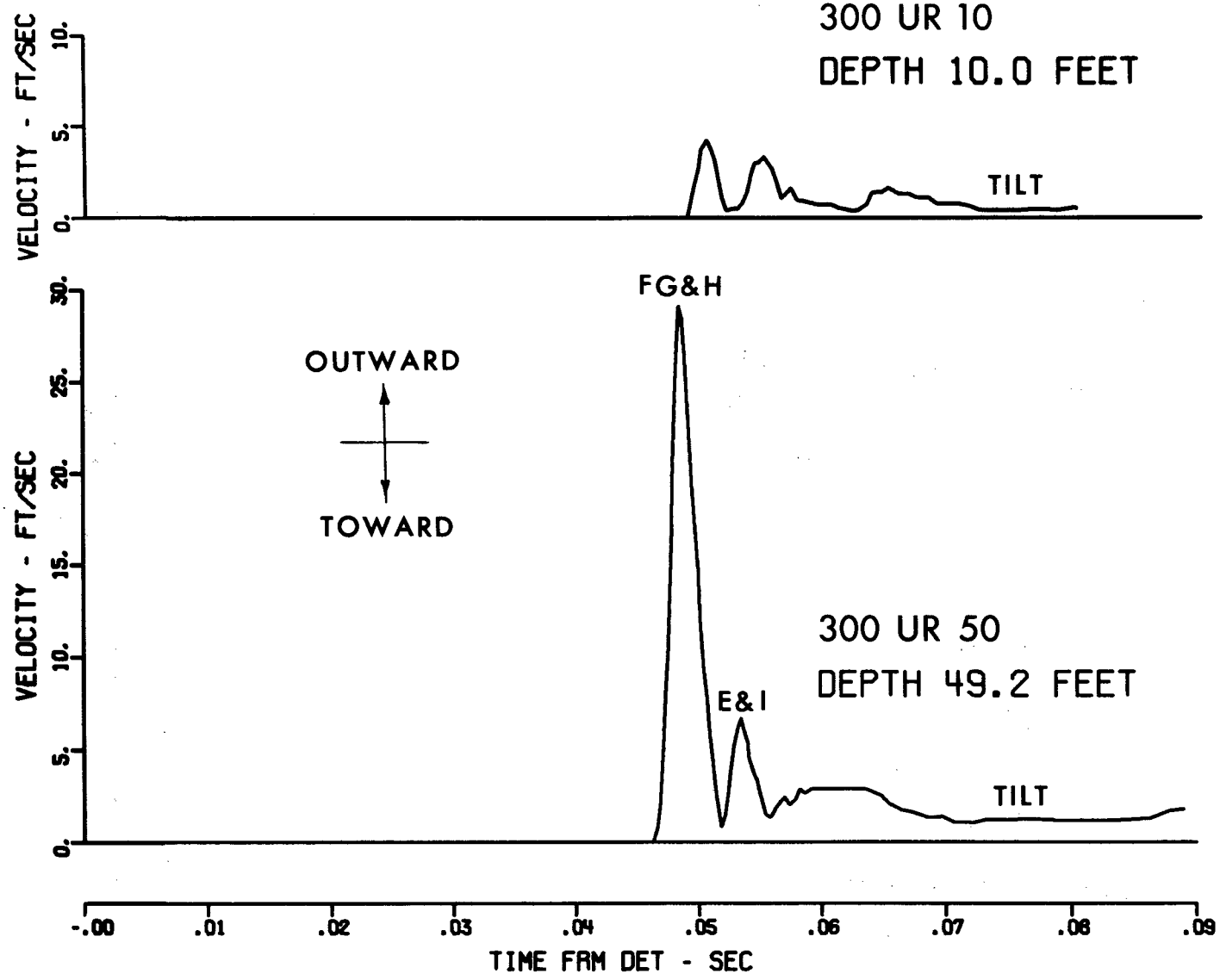

Figure A.11 Radial velocity time histories, Station 300

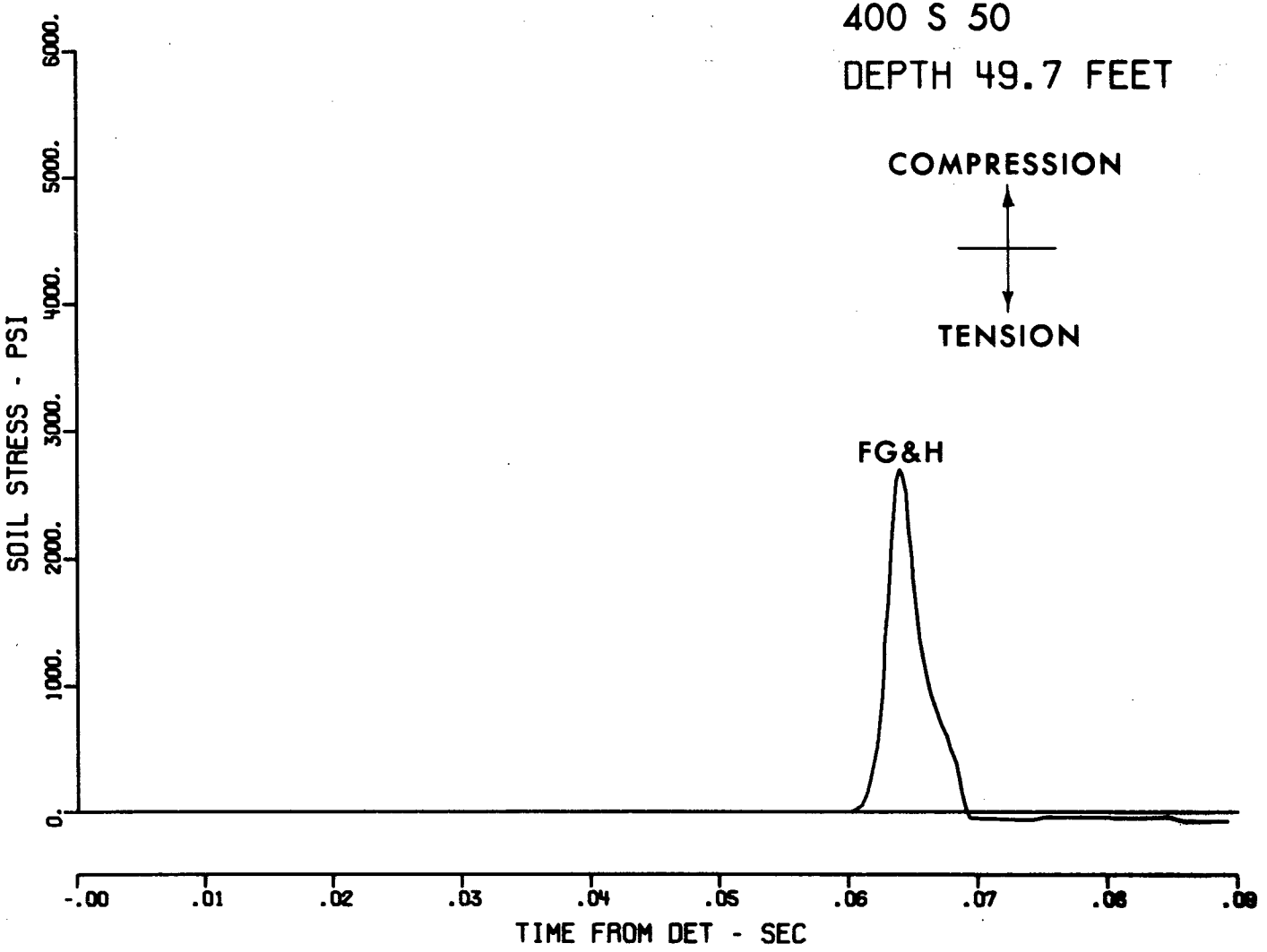

Figure A.12 Stress time history, Station 400

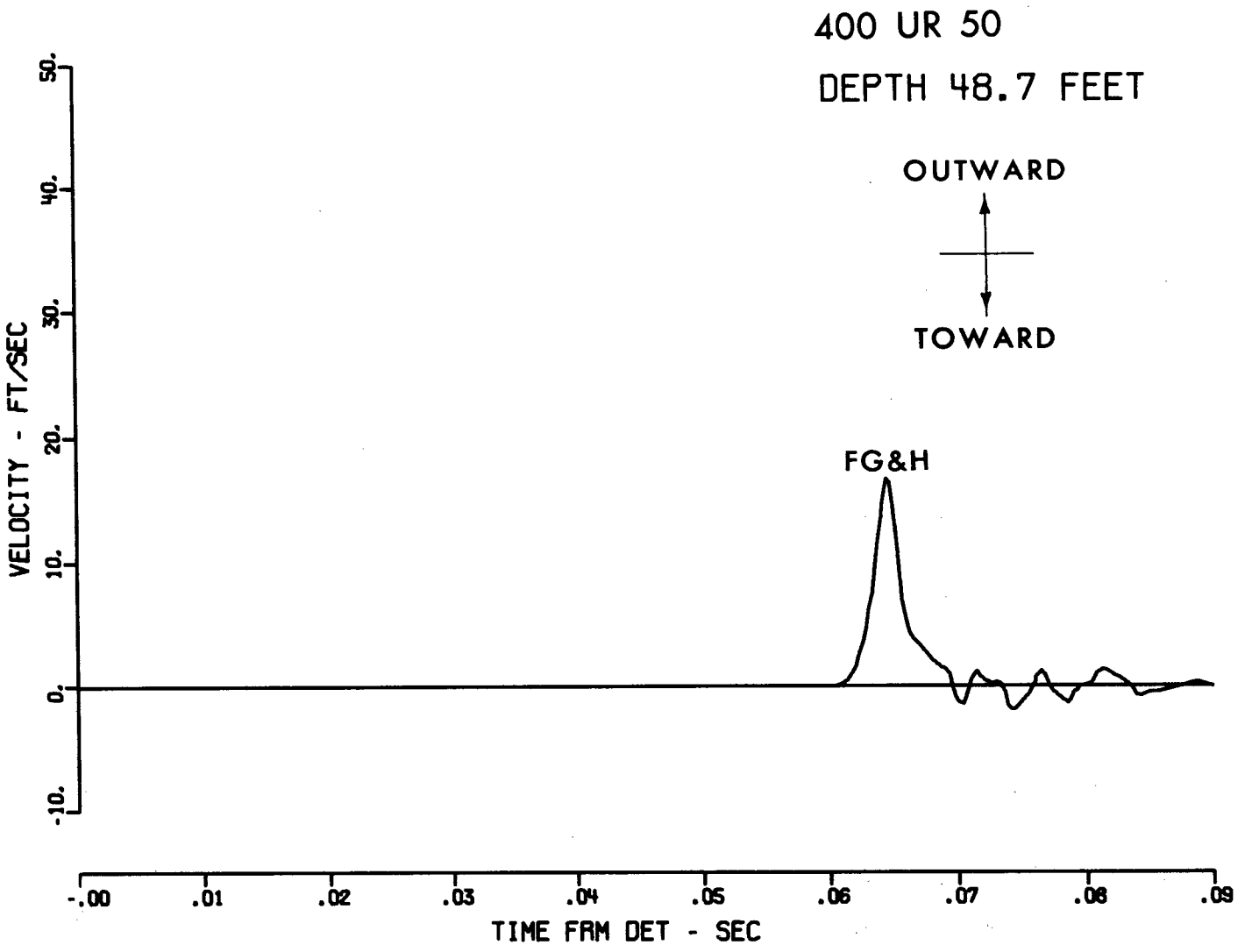

Figure A.13 Radial velocity time history, Station 400

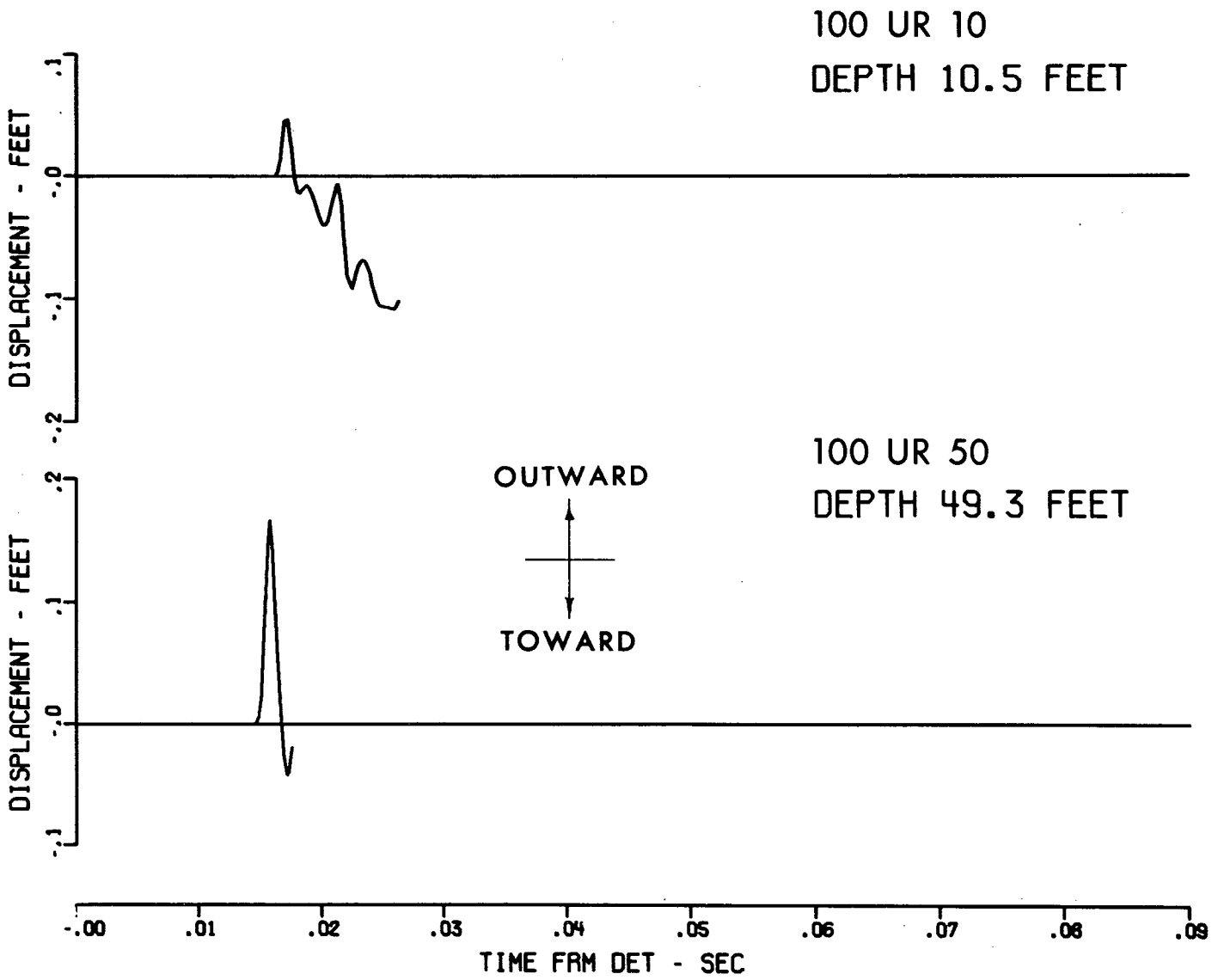

Figure A.14 Computed radial displacement time histories, Station 100

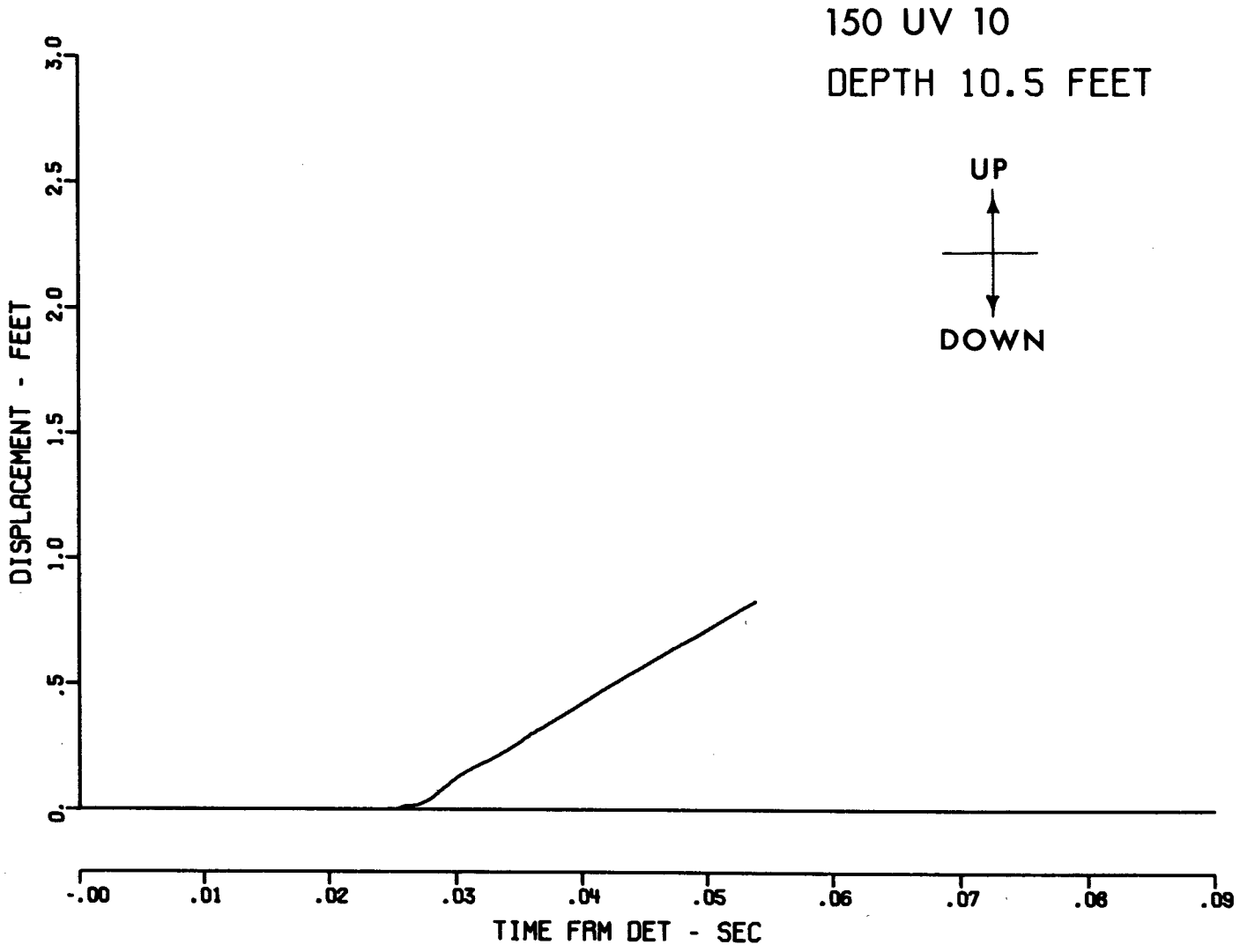

Figure A.15 Computed vertical displacement time history, Station 150

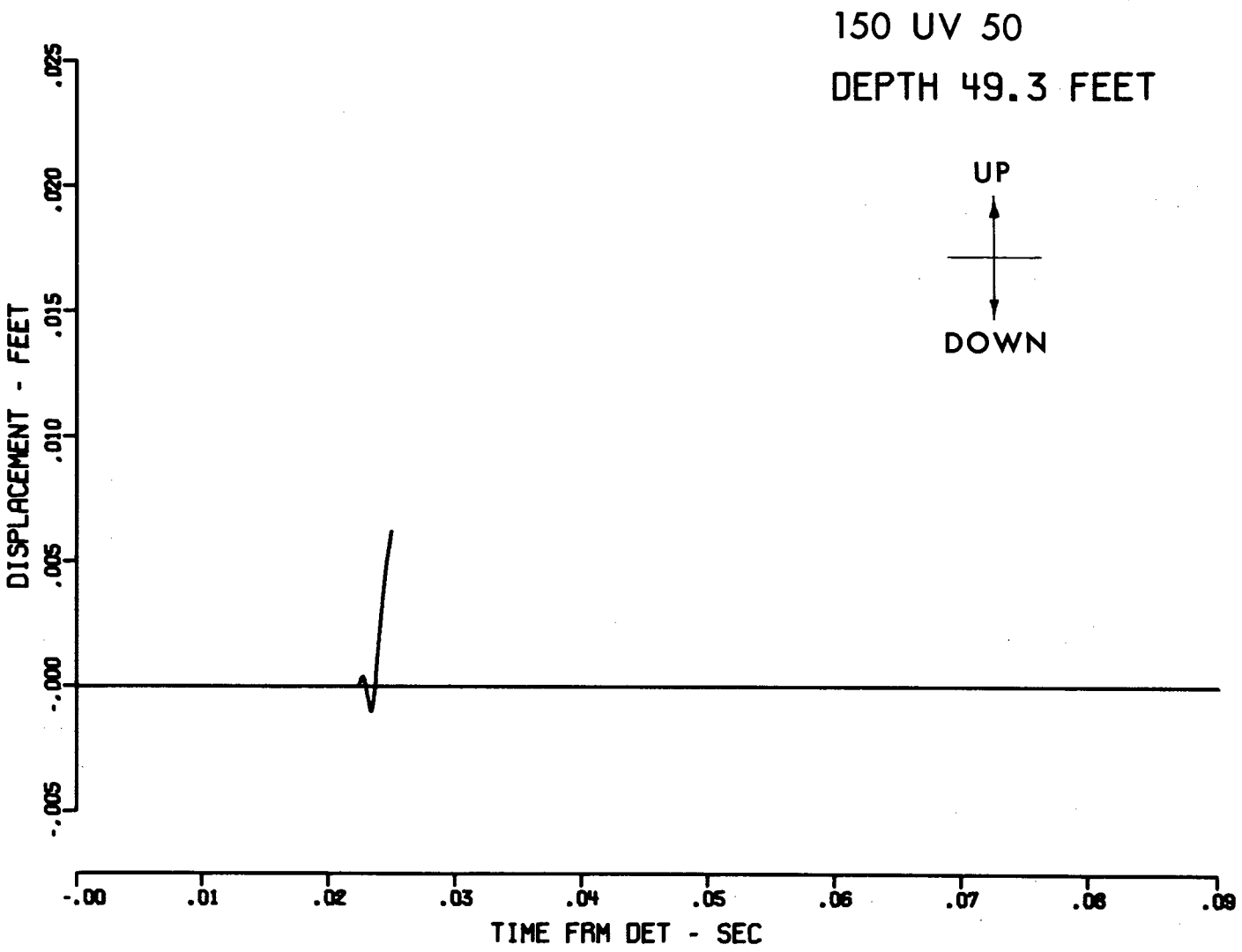

Figure A.16 Computed vertical displacement time history, Station 150

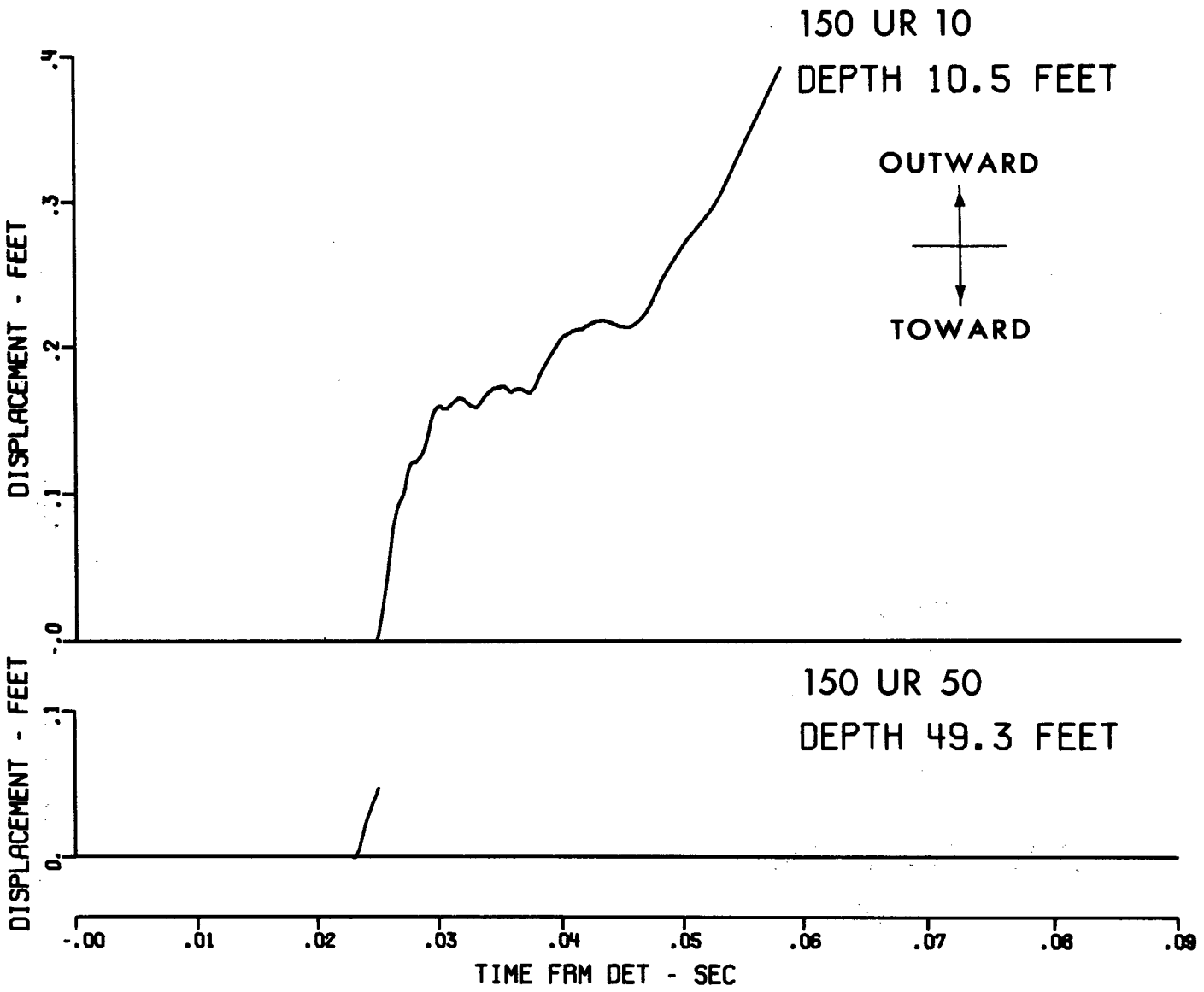

Figure A.17 Computed radial displacement time histories, Station 150

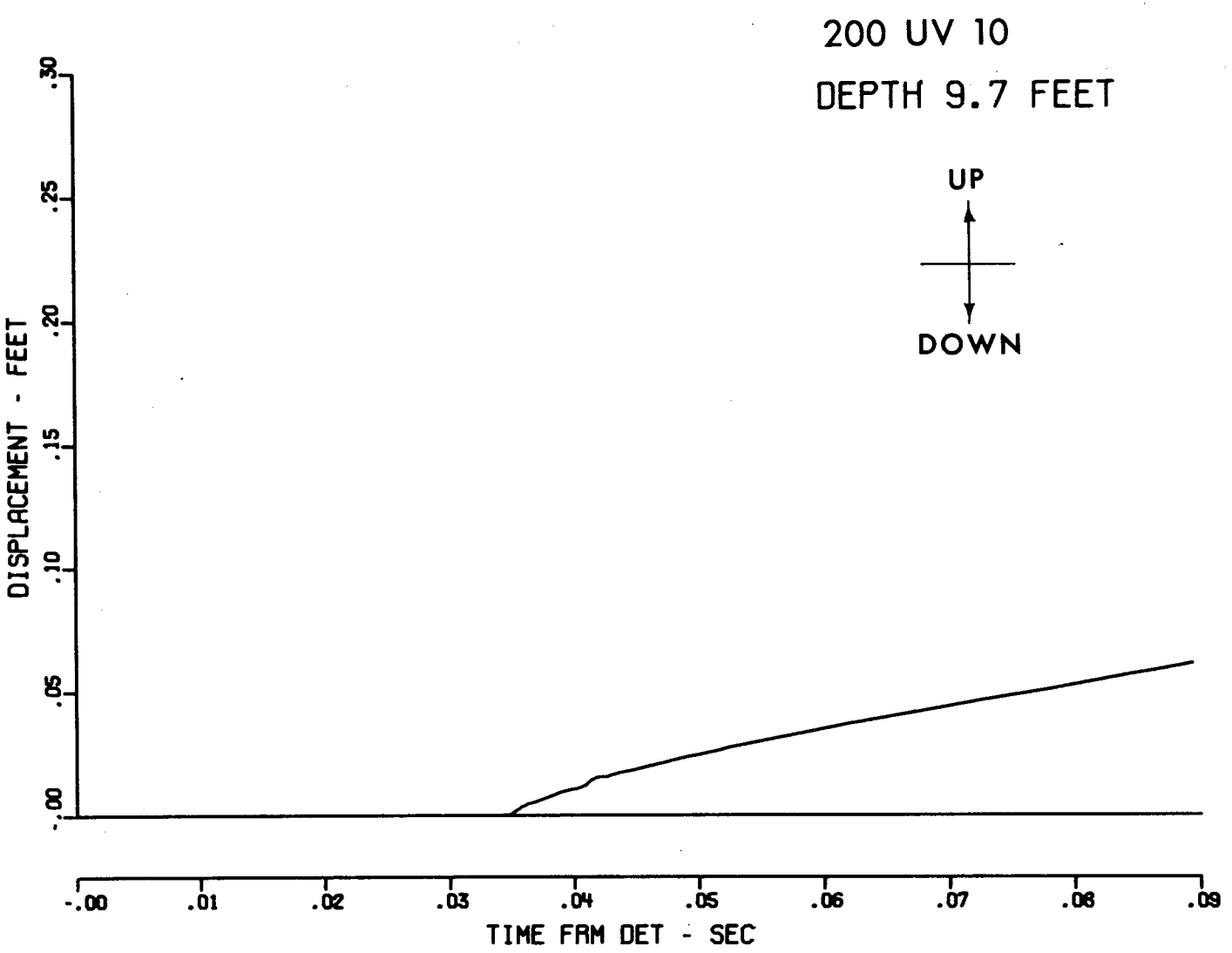

Figure A.18 Computed vertical displacement time history, Station 200

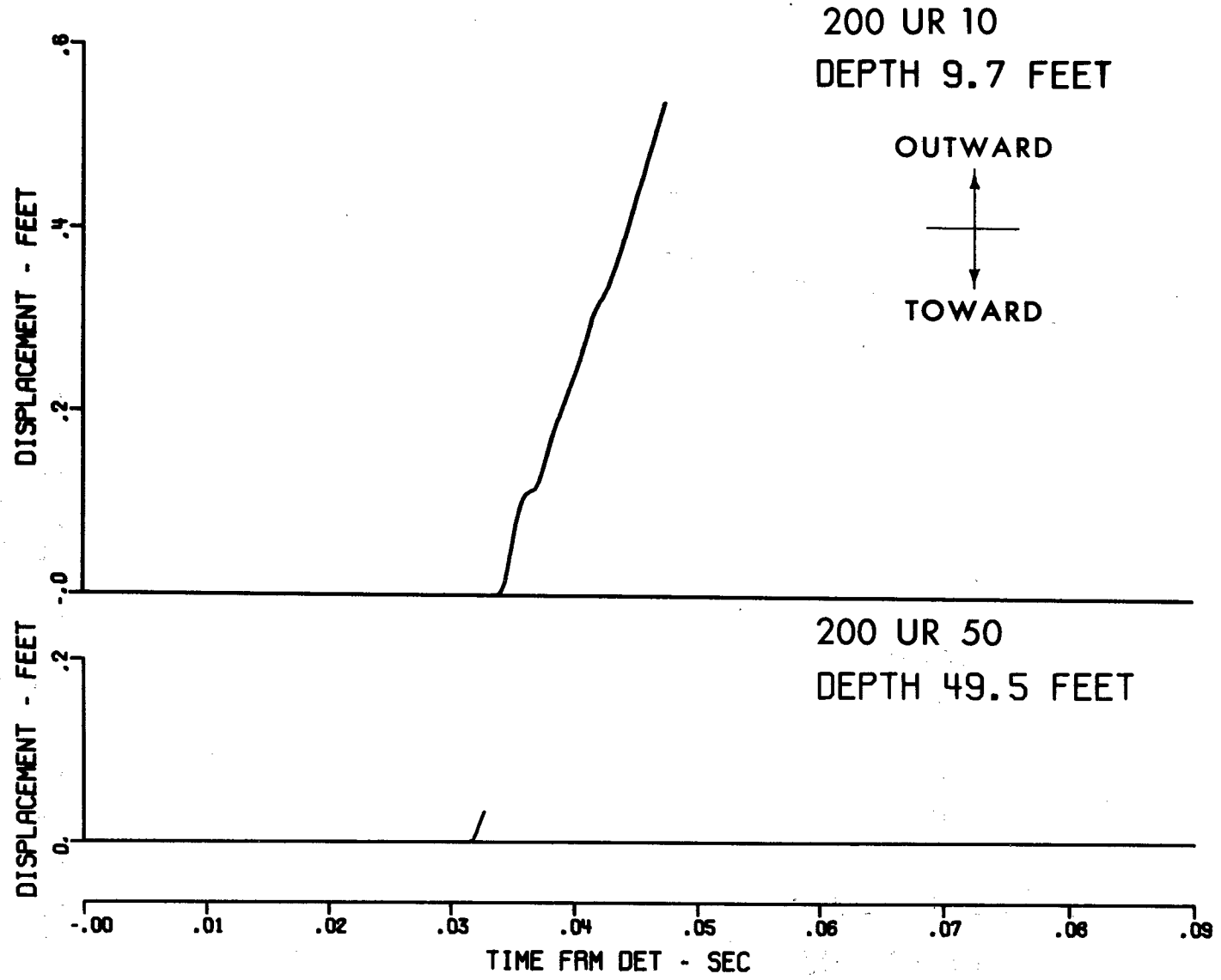

Figure A.19 Computed radial displacement time histories, Station 200

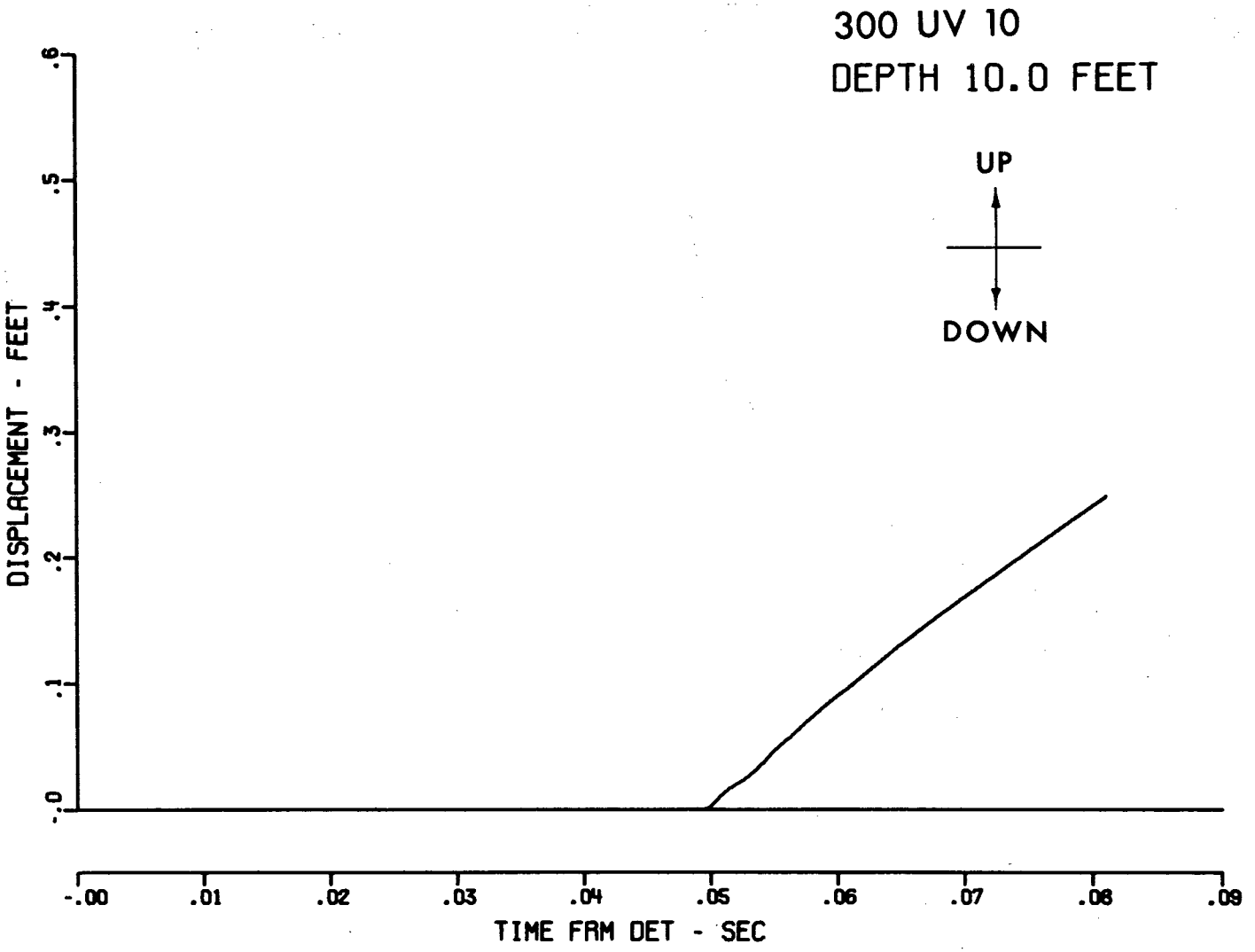

Figure A.20 Computed vertical displacement time histories, Station 300

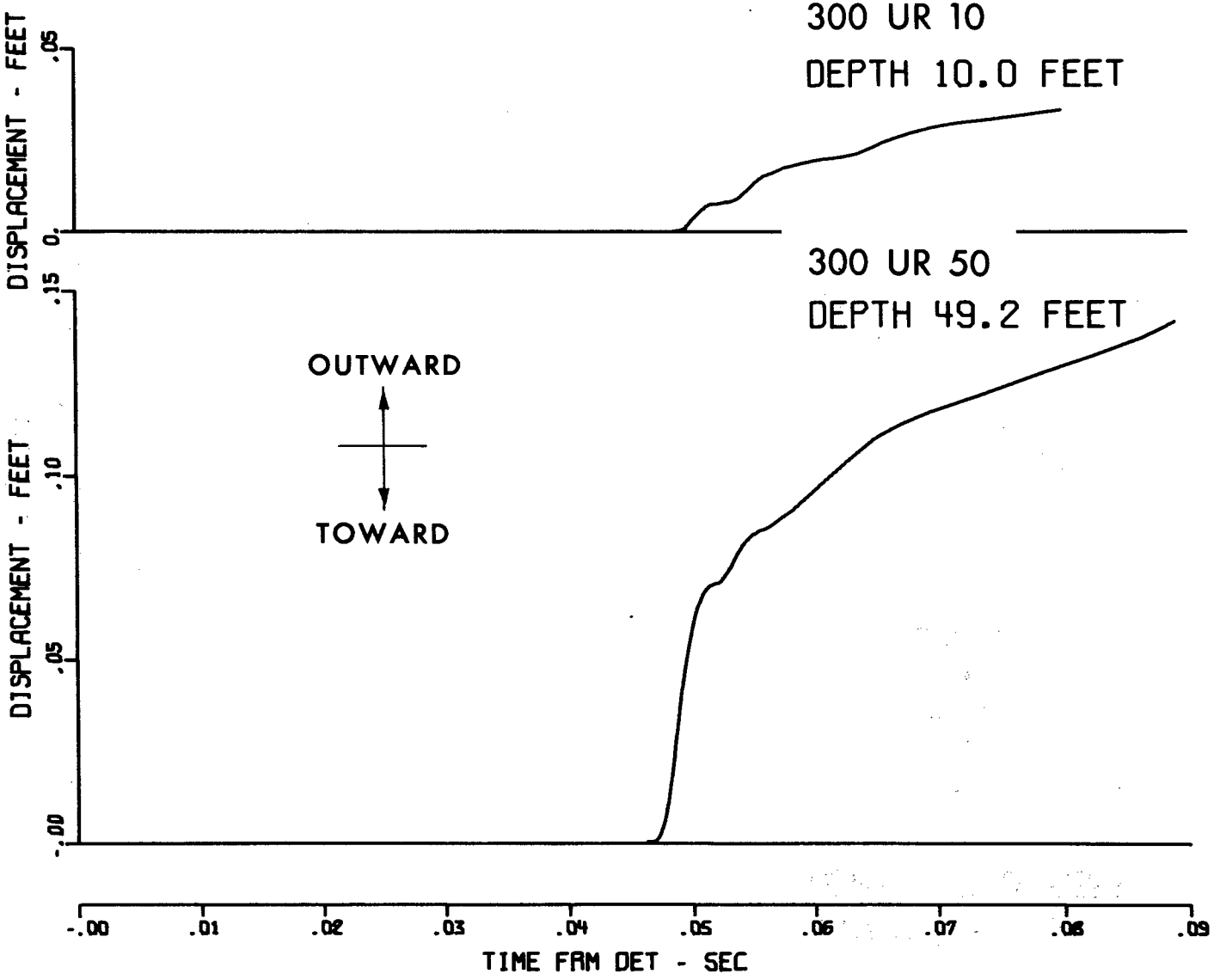

Figure A.21 Computed radial displacement time histories, Station 300

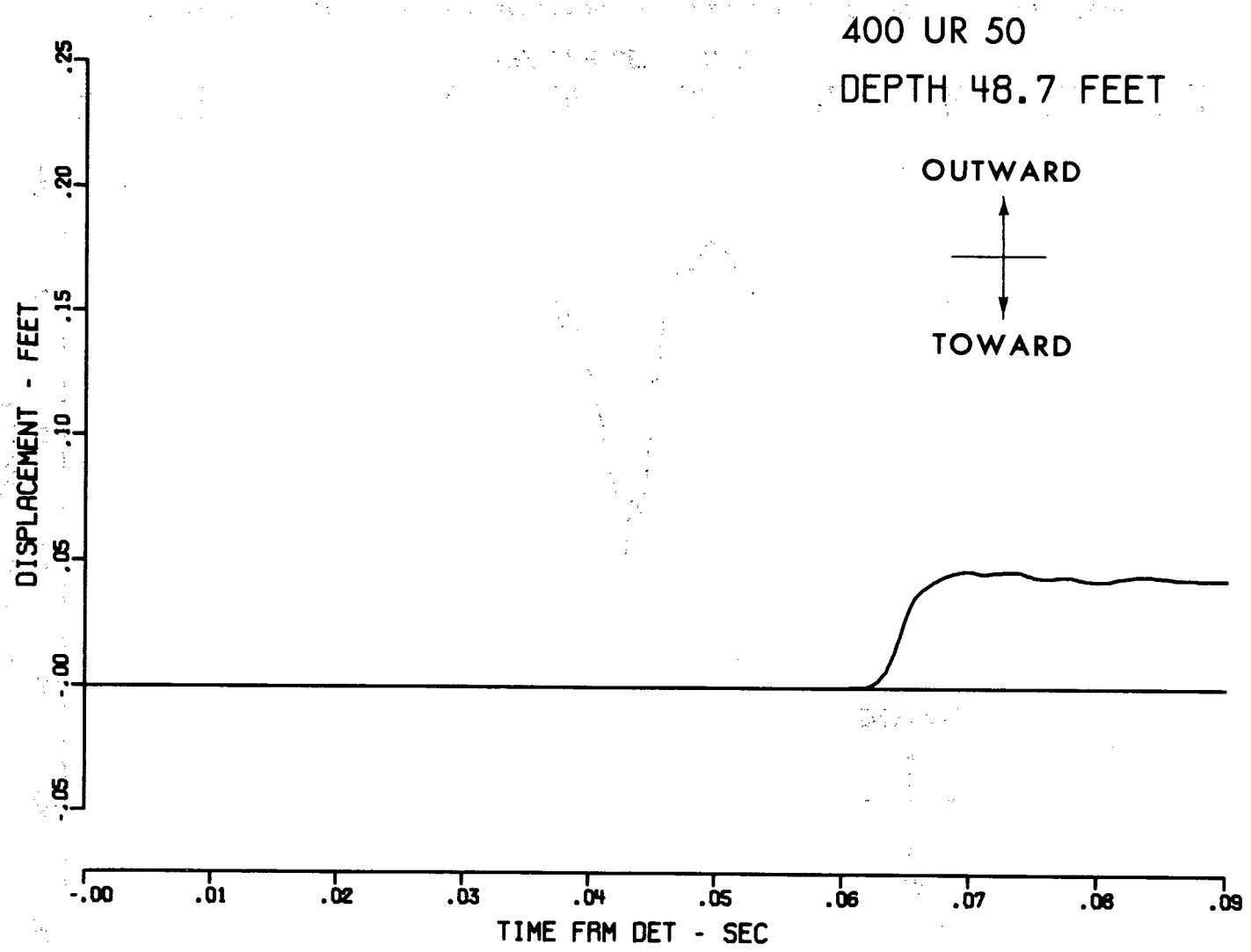

Figure A.22 Computed radial displacement time history, Station 400

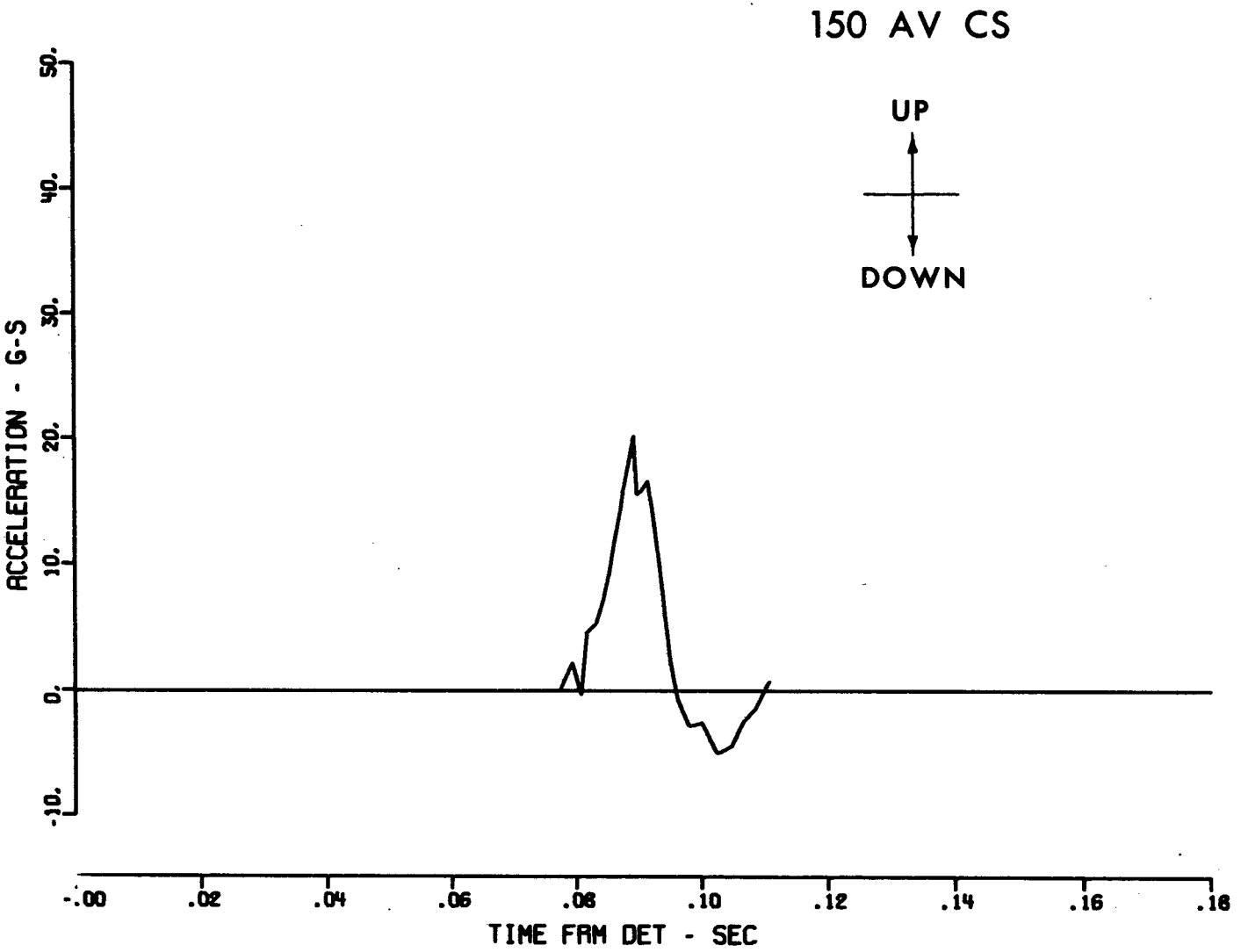

Figure A.23 Vertical acceleration time history on Charlie Crater Slope

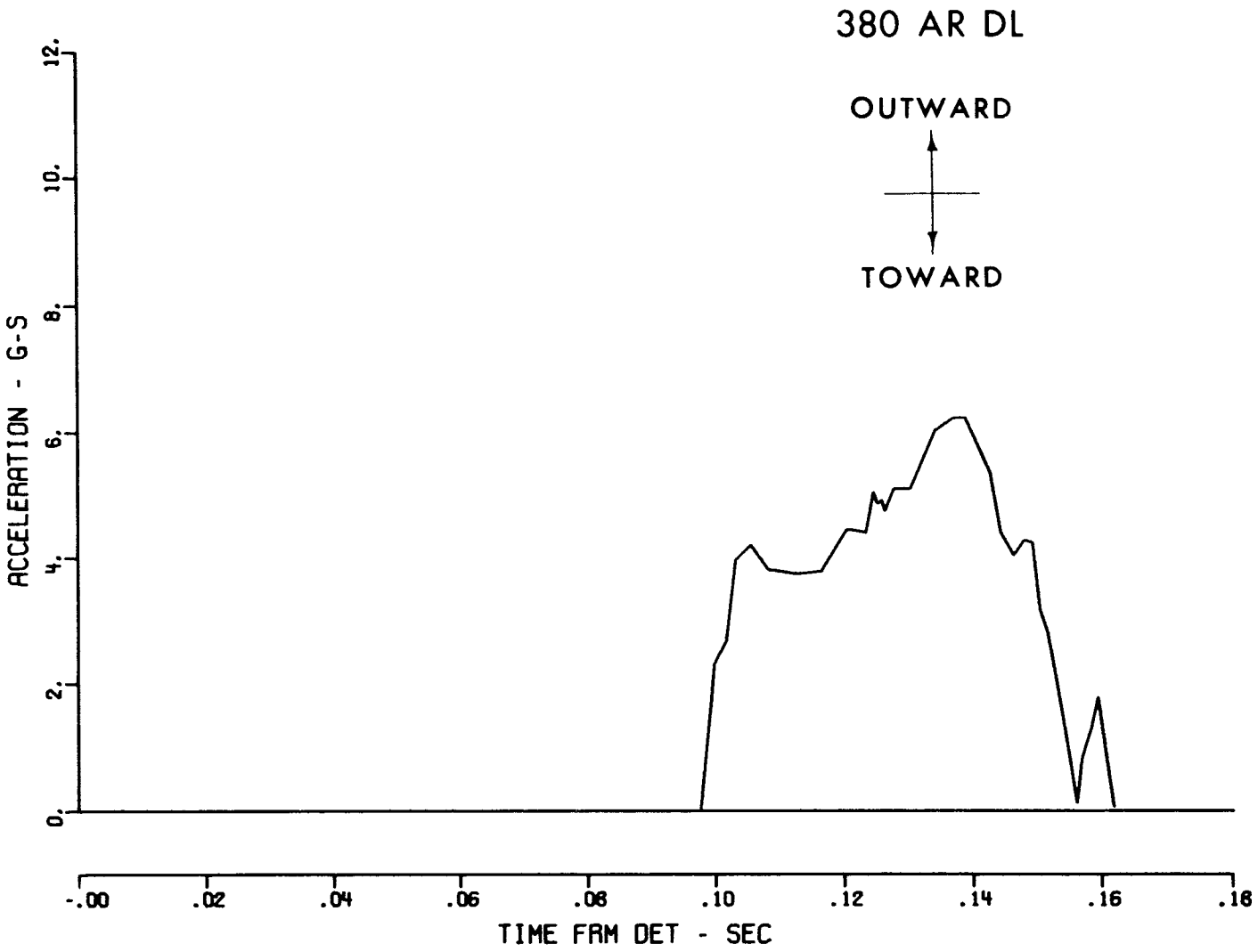

Figure A.24 Radial acceleration time history on Delta Crater Lip

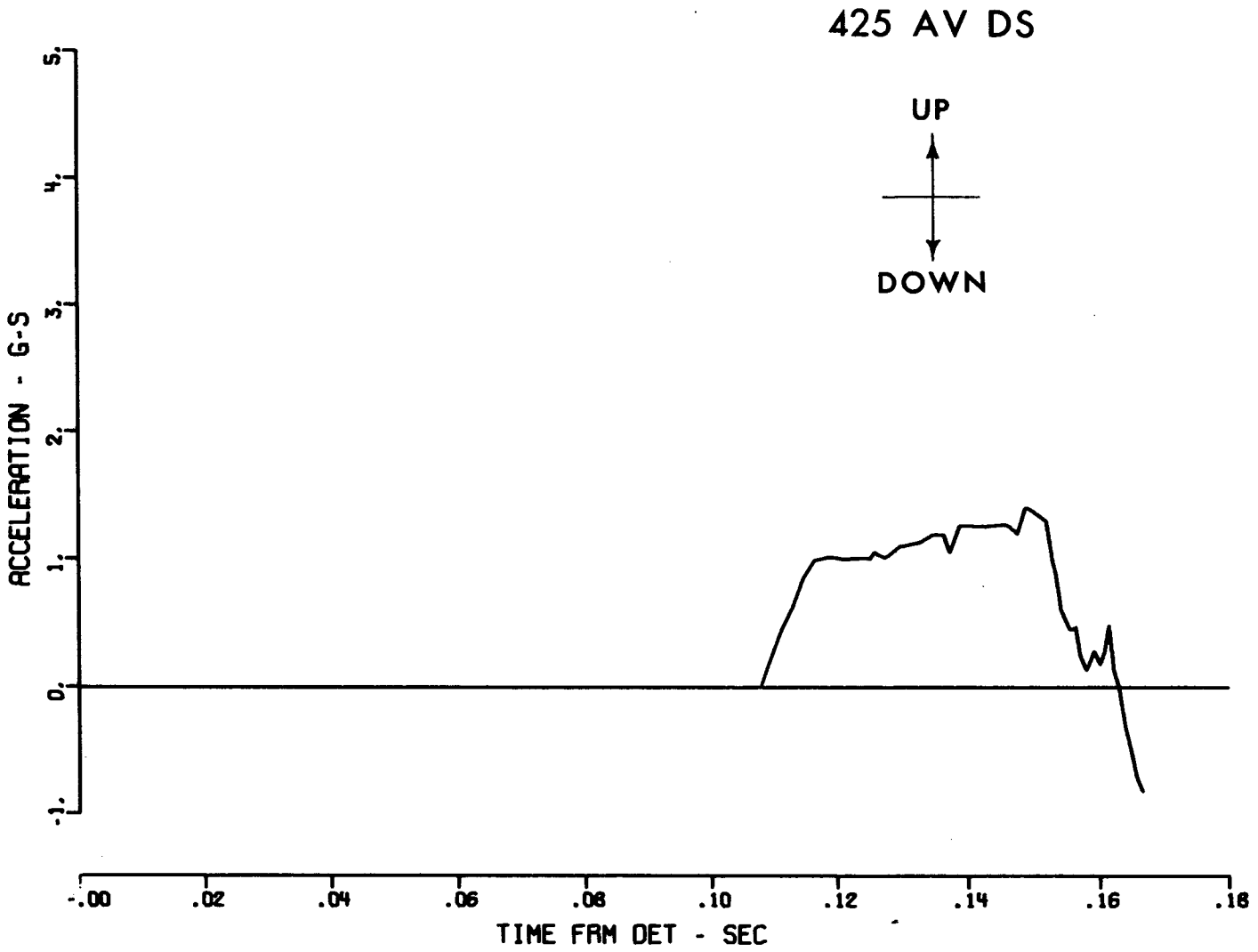

Figure A.25 Vertical acceleration time history on Delta Crater Slope

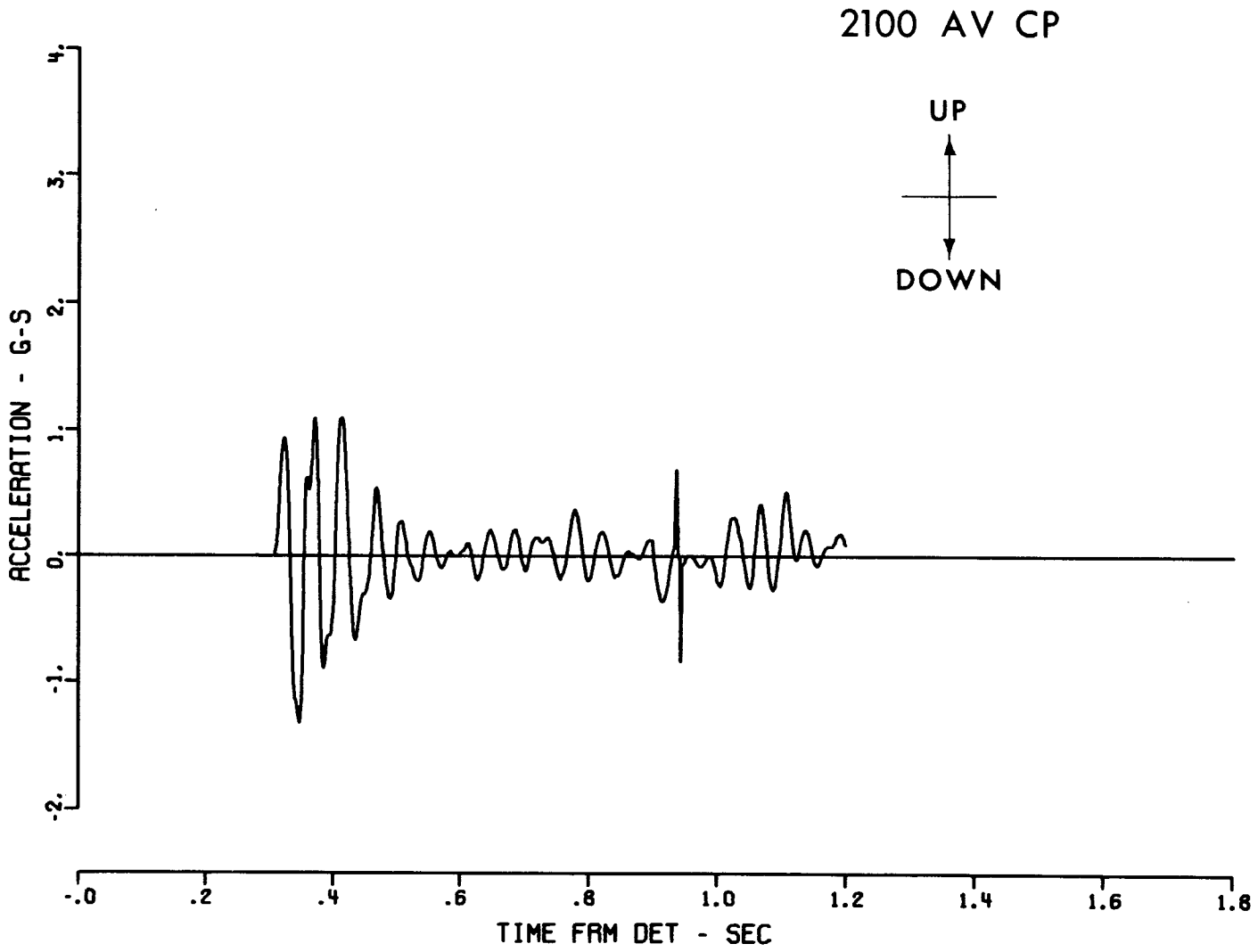

Figure A.26 Vertical acceleration time history at Control Point

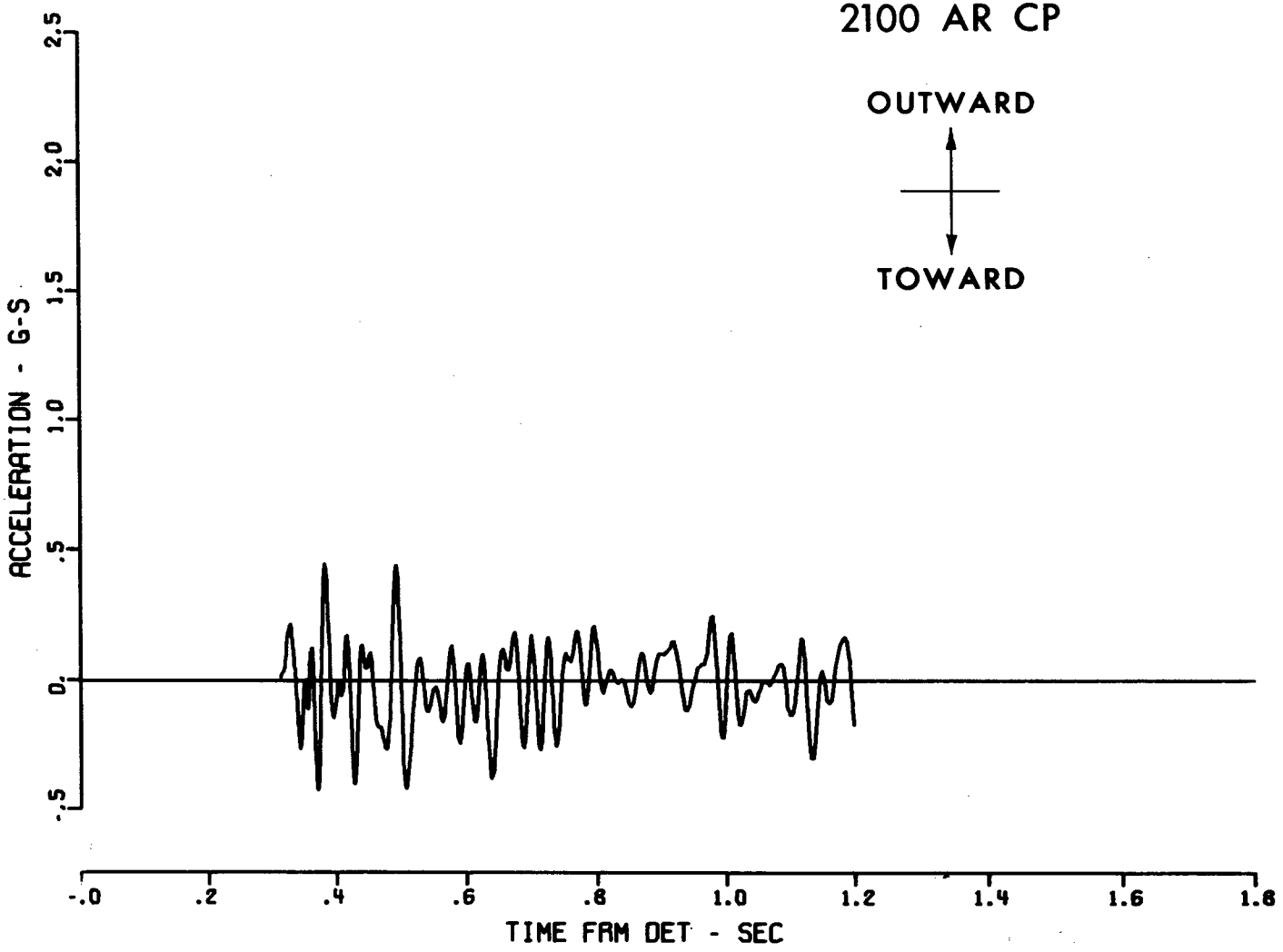

Figure A.27 Radial acceleration time history at Control Point

REFERENCES

1. J. D. Day, D. W. Murrell, W. C. Sherman; "Close-in Ground Motion, Earth Stress, and Pore Pressure Measurements"; Project Pre-GONDOLA I, PNE-1104, September 1967; U. S. Army Engineer Nuclear Cratering Group, Livermore, California.

2. J. D. Day; "Deep Underground Shock Measurements"; Project DUGOUT, PNE-609F, June 1964; U. S. Army Engineer Waterways Experiment Station, Vicksburg, Mississippi.

3. N. M. Newmark and Associates; "Feasibility of Modeling Cavity Behavior in Jointed Rock Masses"; Contract Report 1-135; November 1965.

4. William R. Perret; "Free-Field Ground Motion Studies in Granite"; Operation NOUGAT, Shot Hard Hat, DASA POR-1803, April 1963; Sandia Corporation, Albuquerque, New Mexico.

5. Wendell D. Weart; "Free-Field Earth Motion and Spalling Measurements in Granite"; Vela Uniform Project Shoal, VUF-2001, February 1965; Sandia Corporation, Albuquerque, New Mexico.

6. LTC Maurice K. Kurtz, Jr., and Walter C. Day; "A Report of the Scope and Preliminary Results of Project Pre-GONDOLA II"; 14 August 1967; U. S. Army Engineer Nuclear Cratering Group, Livermore, California.

7. John S. Rinehart; "On Fractures Caused by Explosions and Impacts"; Quarterly of Colorado School of Mines, Volume 55, No. 4, October 1960, Golden, Colorado.

External Distribution	No. copies
D. J. Convey Department of Mines and Technical Surveys Ottawa, Ontario, Canada	
Dr. G. W. Covier Oil and Gas Conservation Board Calgary, Alberta, Canada	
U. S. Army Engineer Division, Lower Mississippi Valley Vicksburg, Mississippi	
Chief of Engineers, ATTN: ENGCW-Z, Washington, D.C.	5
U. S. Army Engineer District, Memphis, Tennessee	
U. S. Army Engineer District, New Orleans, Louisiana	
U. S. Army Engineer District, St. Louis, Missouri	
U. S. Army Engineer District, Vicksburg, Mississippi	
U. S. Army Engineer Division, Mediterranean, Leghorn, Italy	
U. S. Army Engineer District, GULF, Teheran, Iran	
U. S. Army Engineer Division, Missouri River, Omaha, Nebraska	2
U. S. Army Engineer District, Kansas City, Missouri	
U. S. Army Engineer District, Omaha, Nebraska	2
U. S. Army Engineer Division, New England, Waltham, Mass.	
U. S. Army Engineer Division, North Atlantic, New York, N.Y.	
U. S. Army Engineer District, Baltimore, Maryland	
U. S. Army Engineer District, New York, N. Y.	
U. S. Army Engineer District, Norfolk, Virginia	
U. S. Army Engineer District, Philadelphia, Pennsylvania	
U. S. Army Engineer Division, North Central, Chicago, Illinois	
U. S. Army Engineer District, Buffalo, New York	
U. S. Army Engineer District, Chicago, Illinois	
U. S. Army Engineer District, Detroit, Michigan	
U. S. Army Engineer District, Rock Island, Illinois	
U. S. Army Engineer District, St. Paul, Minnesota	
U. S. Army Engineer District, Lake Survey, Detroit, Michigan	
U. S. Army Engineer Division, North Pacific, Portland, Oregon	
U. S. Army Engineer District, Portland, Oregon	
U. S. Army Engineer District, Alaska, Anchorage, Alaska	
U. S. Army Engineer District, Seattle, Washington	

External Distribution (Cont)

U. S. Army Engineer District, Walla Walla, Washington
U. S. Army Engineer Division, Ohio River, Cincinnati, Ohio
U. S. Army Engineer District, Huntington, West Virginia
U. S. Army Engineer District, Louisville, Kentucky
U. S. Army Engineer District, Nashville, Tennessee
U. S. Army Engineer District, Pittsburgh, Pennsylvania
U. S. Army Engineer Division, Pacific Ocean, Honolulu, Hawaii
U. S. Army Engineer District, Far East, San Francisco, Calif.
U. S. Army Engineer District, Honolulu, Hawaii
U. S. Army Engineer District, Okinawa, San Francisco, Calif.
U. S. Army Engineer Division, South Atlantic, Atlanta, Georgia
U. S. Army Engineer District, Canaveral, Merritt Island, Florida
U. S. Army Engineer District, Charleston, South Carolina
U. S. Army Engineer District, Jacksonville, Florida
U. S. Army Engineer District, Mobile, Alabama
U. S. Army Engineer District, Savannah, Georgia
U. S. Army Engineer District, Wilmington, North Carolina
U. S. Army Engineer Division, South Pacific, San Francisco, Calif.
U. S. Army Engineer District, Los Angeles, California
U. S. Army Engineer District, Sacramento, California
U. S. Army Engineer District, San Francisco, California
U. S. Army Engineer Division, Southwestern, Dallas, Texas
U. S. Army Engineer District, Albuquerque, New Mexico
U. S. Army Engineer District, Fort Worth, Texas
U. S. Army Engineer District, Galveston, Texas
U. S. Army Engineer District, Little Rock, Arkansas
U. S. Army Engineer District, Tulsa, Oklahoma
U. S. Army Liaison Detachment, New York, N. Y.
Mississippi River Commission, Vicksburg, Mississippi
Rivers and Harbors, Boards of Engineers, Washington, D. C.
Corps of Engineers Ballistic Missile Construction Office
Norton Air Force Base, California
U. S. Army Engineer Center, Ft. Belvoir, Virginia
U. S. Army Engineer School, Ft. Belvoir, Virginia
U. S. Army Engineer Reactors Group, Ft. Belvoir, Virginia

External Distribution (Cont)	No. of Copies
U. S. Army Engineer Training Center, Ft. Leonard Wood, Missouri	
U. S. Coastal Engineering Research Board, Washington, D.C.	
U. S. Army Engineer Waterways Experiment Station, Vicksburg, Mississippi	50
U. S. Army Engineer Nuclear Cratering Group, Livermore, California	75
TID-4500, UC-35, Nuclear Explosions - Peaceful Applications	259

LRL Internal Distribution

Michael M. May
R. Batzel
J. Gofman
R. Goeckermann
C. Haussmann
J. Rosengren
D. Sewell
C. VanAtta
C. McDonald
E. Goldberg
G. Higgins
J. Carothers
S. Fernback
J. Hadley
J. Kane
B. Rubin
J. Kury
P. Stevenson
J. Bell
E. Hulse
W. Decker
W. Harford
G. Werth
M. Nordyke
F. Holzer
H. Tewes
J. Toman (2)
J. Knox
R. K. Wakerling, Berkeley
J. Kahn
E. Teller, Berkeley
D. M. Wilkes, Berkeley
L. Crooks, Mercury
TID File (10)
H. L. Reynolds
P. Molthrop
F. Eby
T. Cherry
R. Terhune